Insights into flood-dominated fan-deltas: very high-resolution seismic examples off the Amalfi cliffed coasts, eastern Tyrrhenian Sea

M. Sacchi, F. Molisso, C. Violante, E. Esposito, D. Insinga, C. Lubritto, S. Porfido and T. Tóth

---

Email alerting service	click here to receive free email alerts when new articles cite this article
Permission request	click here to seek permission to re-use all or part of this article
Subscribe	click here to subscribe to Geological Society, London, Special Publications or the Lyell Collection

---

Notes

Insights into flood-dominated fan-deltas: very high-resolution seismic examples off the Amalfi cliffed coasts, eastern Tyrrhenian Sea

M. SACCHI[1]*, F. MOLISSO[1], C. VIOLANTE[1], E. ESPOSITO[1], D. INSINGA[1],
C. LUBRITTO[2], S. PORFIDO[1] & T. TÓTH[3,4]

[1]*Istituto per l'Ambiente Marino Costiero (IAMC)—CNR, Napoli, Calata P.ta di Massa,
Porto di Napoli, 80133—Napoli, Italy*

[2]*Dipartimento di Scienze Ambientali, Seconda Università di Napoli, Via Vivaldi,
43—81100 Caserta, Italy*

[3]*Department of Geophysics, Eötvös Loránd University, Pázmány Péter sétány 1/C,
H-1117 Budapest, Hungary*

[4]*Present address: Geomega Ltd., Mester u. 4, 1095 Budapest, Hungary*

*Corresponding author (e-mail: marco.sacchi@iamc.cnr.it)

Abstract: A high-resolution (IKB-Seistec) seismic survey calibrated with gravity-core data, off the Amalfi coast, a rocky coastal area on the southern side of the Sorrento Peninsula (Italy), documents the internal stratigraphic architecture of a series of small fan-deltas that develop at the mouth of major bedrock streams. The fan-delta system mostly postdates the Plinian eruption of Vesuvius of AD 79 and displays various phases of development associated with periods of high sediment supply from the adjacent river basins. During these periods landscape-mantling loose pyroclastic deposits (mostly air-fall tephra from Vesuvius) were quickly eroded and delivered to the continental shelf by sheet wash and flash flood events. Depositional processes on the foresets were dominated by sediment gravity flows originating from hyperpycnal river flow and pyroclastic fall deposits. This in turn created favourable conditions for sea-floor instability, soft sediment failure, slumping and sliding, which characterize the deltaic stratigraphic architecture. The intermittently increased sediment yield during the various phases of the evolution of the fan-delta system was probably influenced also by the morphoclimatic regime. This may have resulted in varying rates of progradation of the delta foresets, tentatively correlated with the main climatic oscillations of the last 2000 years. The Amalfi fan-delta system represents a small-scale analogue for larger flood-dominated fan-deltas of the world and may be regarded as a useful example for a better understanding of inner-shelf, mixed siliciclastic–volcaniclastic fan-delta systems in the stratigraphic record.

In recent years, deltaic depositional settings at the mouth of small rivers of the Mediterranean and other temperate regions have received growing attention, because of the relevance of these facies associations in the understanding of the late Quaternary evolution of inner-shelf depositional systems and their interaction with fluvio-deltaic processes, sea-floor instability of delta slopes, coastal volcanism, active tectonics, and the climatic regime (Nava-Sanchez *et al.* 1999; Sacchi *et al.* 2005; Trincardi & Syvitski 2005; Lobo *et al.* 2006; McConnico & Bassett 2007).

The renewed interest in fan-deltas has partly derived from the recognition that deltas are unstable sedimentary systems prone to severe physiographic changes (e.g. modification of the coastline or sea-floor instability) that may occur on human time scales. Recent research has been particularly focused on sea-floor failures that are common both on continental slopes and in some deltaic settings; they can represent a major threat not only to oil and other offshore installations but also to the marine environment and coastal facilities. Moreover, in recent years sedimentologists have returned to modern fan-deltas as a possible source of reliable criteria for the recognition of fan-delta deposits in the stratigraphic record (Nemec & Steel 1988; Colella & Prior 1990; Nemec 1990*a*; Wescott & Ethridge 1990).

There is a large variability of underwater fan-delta architecture, depending on the process combinations and the relative dominance of each. Differences in types and rates of sediment supply and the onshore morphology influence underwater delta growth. Sediment dispersal underwater is directly related to supply by rivers. In the case of

bedrock rivers and streams of temperate regions that form fan-deltas along high-relief sea-cliffed coasts (Nava-Sanchez *et al.* 1999; Fernández-Salas *et al.* 2003; Hasiotis *et al.* 2006; Lobo *et al.* 2006; Violante 2009; Violante *et al.* 2009), the fluvial regime is basically controlled by episodic, but sometimes catastrophic discharges that cause flooding on the fans. Long-term development of fan-deltas obviously involves a wide range of possible processes but variations in sediment supply and in the morphoclimatic regime appear to be major controls (e.g. Colella & Prior 1990; Reading 1996; Einsele 2000).

It has long been recognized that the fronts of marine deltas are prone to failure of unconsolidated sediments, and in some cases are dominated by products of mass movements deriving from instability of the delta front (Coleman & Prior 1982; Lindsay *et al.* 1984; Coleman 1988). The main reasons for sediment-induced deformation include: (1) the relatively high sedimentation rate on the delta front, which causes undercompaction and high pore-fluid pressures or liquefaction, leading in turn to loss of shear strength within the deposits; (2) biodegradation of organic debris and associated free methane gas, which weakens the sediment stability; (3) shocking of accumulated sediment by storm and wave action; (4) sediment instability induced by earthquakes.

Among the factors that may have a significant impact on fan-delta construction, and eventually sea-floor instability at the delta front and slopes are, hence, the frequency of recurrence of exceptional river floods, mudflows and explosive eruptions (involving pyroclastic falls, surges and flows) of coastal volcanoes. These processes can all induce the supply of large volumes of loose or poorly consolidated sediment into the delta system and over vast areas of the continental shelf (Cinque *et al.* 1997; Major *et al.* 2000; Lirer *et al.* 2001; Sacchi *et al.* 2005; Sulpizio *et al.* 2006; Bisson *et al.* 2007; Cinque & Robustelli 2009).

This paper focuses on the sequence stratigraphic interpretation of high-resolution seismic and gravity-core data acquired on a series of small fan-deltas that have developed on the inner shelf of the Amalfi coast. The aim of the study is the detailed reconstruction of stratal architecture of the fan-deltas and the interpretation of seismic facies in terms of depositional processes and environmental setting. The application of ultra high-resolution seismic data to inner-shelf and small-scale fan-deltas in shallow water provides unprecedented detailed insights into shallow-water depositional systems, documenting sea-floor morphology and areas of active erosion or deposition, allowing for bed-to-bed correlation in the gravity-core calibration of the seismic record.

Geological setting

The eastern Tyrrhenian margin is characterized by a number of peripheral basins that evolved during the latest Neogene–Quaternary across the hinge zone between the southern Apennines fold and thrust belt and the Tyrrhenian back-arc extensional area (Fig. 1). These basins, which include the present-day Bay of Salerno, formed in response to large-scale orogen-parallel extension and associated transtensional tectonics that accompanied the anti-clockwise rotation of the Apennine belt and lithospheric stretching in the central Tyrrhenian basin (Malinverno & Ryan 1986; Oldow *et al.* 1993; Sacchi *et al.* 1994; Ferranti *et al.* 1996; Patacca & Scandone 2007). Quaternary orogen-parallel extension caused the formation of half-graben systems (e.g. Bay of Naples, Bay of Salerno) and intervening structural highs (e.g. Sorrento Peninsula) that are perpendicular to the main axis of the Apennine thrust belt (Bartole *et al.* 1984; Mariani & Prato 1988; Sacchi *et al.* 1994; Milia & Torrente 1999; Acocella & Funiciello 2006). The extensional processes caused in turn the onset of intense volcanism. Active volcanic centres are represented by Somma–Vesuvius, the island of Ischia and the district of the Campi Flegrei, with its numerous vents both onshore and offshore the Bay of Naples (Rosi & Sbrana 1987; Santacroce 1987; Vezzoli 1988; Milia *et al.* 1998; Santacroce & Sbrana 2003).

The Sorrento Peninsula

The study area is located on the southern slope of the Sorrento Peninsula (Amalfi coast). The peninsula is a major Quaternary morpho-structural unit of the western flank of the Southern Apennines and forms a narrow and elevated mountain range (up to 1444 m) that separates two major embayments of the eastern Tyrrhenian margin, namely the Bay of Naples and the Bay of Salerno. It is mostly formed by a pile of Mesozoic carbonate rocks, covered by Tertiary to Quaternary siliciclastic and pyroclastic units, and is deeply cut by a complex of bedrock rivers and channels characterized by relatively small catchment areas and pronounced disequilibrium of the stream profiles (Fig. 2). These rivers have flow that shows a distinct seasonality and a torrential behaviour (Esposito *et al.* 2004*a*, *b*; Budillon *et al.* 2005; Liquete *et al.* 2005; Violante *et al.* 2009); their source is very high relative to the base level, and erosion processes have proceeded rapidly and generated a rugged morphology (Reineck & Singh 1975; Einsele 2000).

Being a horst-like structure in a half-graben basin setting the Sorrento Peninsula displays a remarkable asymmetry in the morphology of its two flanks, the southern one (Amalfi coast) being
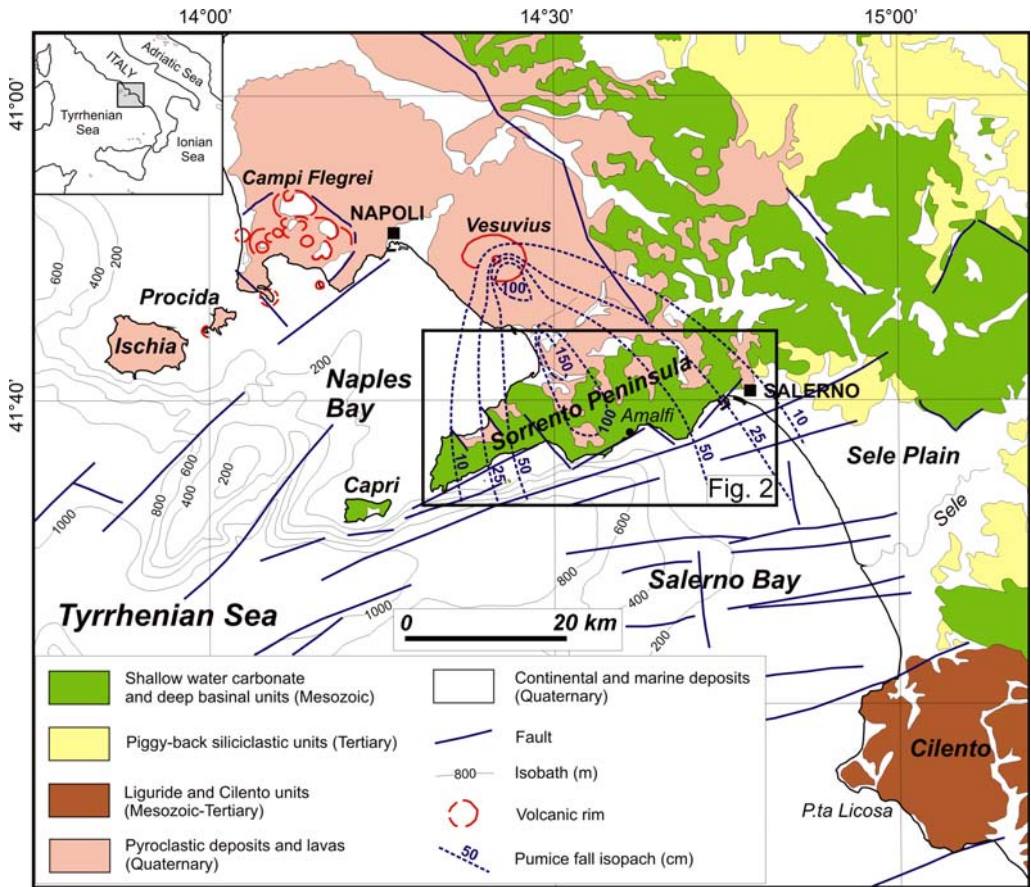
Fig. 1. Tectonic sketch-map of the Campania continental margin (eastern Tyrrhenian Sea) and location of the study area (Amalfi coast of the Sorrento Peninsula).
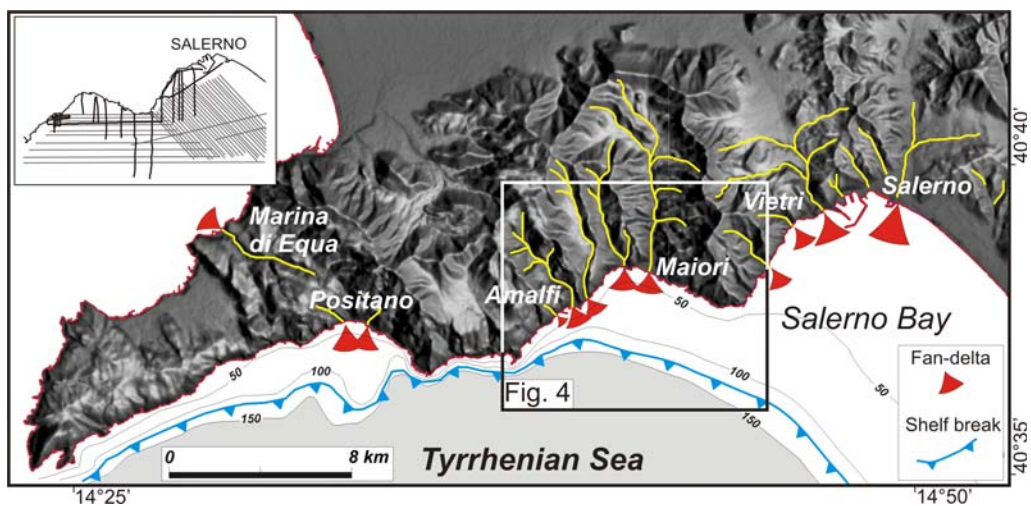

Fig. 2. Shaded relief map of the Sorrento Peninsula and location of the fan-delta systems fed by the main streams of the Amalfi coast. Box shows location of Figure 4. Inset shows the full seismic database used for this research.

steeper and narrower than the northern one (Sorrento coast). This asymmetry can also be observed offshore, where the narrow continental shelf on the Amalfi side contrasts with a wider shelf in the southern part of the Bay of Naples. As a consequence the Amalfi flank of the peninsula is characterized by tectonically uplifted rocky and steep backdrops, deeply incised gorges, and coastal cliffs (Brancaccio *et al.* 1991).

Coarse-grained coastal alluvial fans confined by narrow valleys at the mouth of the major streams are relatively common in this setting (Fig. 2). They are formed by deposition from flash floods, during periods of heavy rainfall. The delivery of sediments towards the coastal fans is favoured by the steep slopes and the loose source-area material of a wide size range (diameters vary from 2 m or more down to clay size) that includes bedrock river gravel, slope-weathering products, soil and unconsolidated volcaniclastic deposits.

Landscape-mantling pyroclastic deposits and the recent volcanic activity of Somma–Vesuvius

The Sorrento Peninsula, located about 20 km south of Somma–Vesuvius, has been repeatedly mantled during recent millennia by the pyroclastic products of the volcano, which has alternated intense phases of explosive activity accompanied by emission of fine ashes with periods of quiescence (Santacroce 1987). The Late Holocene activity of Somma–Vesuvius includes the Plinian event of the 'Avellino Pumice' and six inter-Plinian events (AP1–AP6; Andronico & Cioni 2002) during the nearly 1600 year period preceding another Plinian event ('Pompeii Pumice'), which destroyed the Roman cities of Pompeii, Stabiae and Herculaneum in AD 79 (Fig. 3).

The volume of the Pompeii fall products has been estimated between 4 km^3 (Sigurdsson *et al.* 1985) and 1–1.5 km^3 (Cioni *et al.* 1999) of Dense Rock Equivalent (DRE). Following the eruptive event, the Sorrento Peninsula was covered by up to 2 m of pyroclastic air-fall tephra (Lirer *et al.* 1973; Sigurdsson *et al.* 1985; Carey & Sigurdsson 1987; Cioni *et al.* 1992). This exceptionally high thickness of pyroclastic fall deposits was due to both the large volume of the erupted products and the main direction of dispersal of the air-fall tephra towards the SW, possibly as a consequence of the direction of dominant winds during the eruptive event (see Fig. 1). Deposits related to the so-called 'Pompeii' eruption have been recognized offshore (Carbone *et al.* 1984; Buccheri *et al.* 2002; Insinga 2003; Munno & Petrosino 2004). More recently a detailed description of the proximal

deposits in the Bays of Naples and Salerno was reported by Sacchi *et al.* (2005), Insinga *et al.* (2008) and Milia *et al.* (2008).

The three centuries of activity following the AD 79 eruption were characterized by the emission of ash ('S. Maria Cycle', Andronico *et al.* 1995) until two sub-Plinian events that occurred in AD 472 (the so-called 'Pollena' eruption of Rosi & Santacroce 1983; Santacroce 1987; Rolandi *et al.* 2004; Sulpizio *et al.* 2005) and in AD 512. Intense activity, including four major eruptions the ('Medieval' events of Rolandi *et al.* 1998), characterizes the history of Somma–Vesuvius up to the 12th century. Products related to this period cover a wide area in the eastern and southeastern sector of the volcano both on land (Rolandi *et al.* 1998; Santacroce & Sbrana 2003) and offshore in the Bay of Naples (Insinga *et al.* 2008).

Following the AD 1631 sub-Plinian eruption (Rolandi *et al.* 1993; Rosi *et al.* 1993), the volcano experienced a 300 year period of semi-persistent, mild activity with a total volume of erupted material of the order of 10^7 m^3 (Arrighi *et al.* 2001). During this period only a few eruptions reached sub-Plinian intensity (e.g. in 1822 and 1906) and only five events were accompanied by a violent phreatomagmatic phase (i.e. in 1779, 1794, 1822, 1906 and 1944; Arrighi *et al.* 2001).

The explosive eruptions of Somma–Vesuvius in recent millennia have repeatedly accumulated loose pyroclastic material over large areas of the Campania region, thus creating favourable conditions for volcaniclastic debris to generate mass flows on slopes (Sulpizio *et al.* 2006; Bisson *et al.* 2007).

The Amalfi continental shelf

The continental shelf in the Bay of Salerno extends for about 70 km from the island of Capri in the north to Punta Licosa in the south. It is characterized by a varied morphology, controlled by both the tectonic activity and uplift of the Sorrento Peninsula and the associated high sediment supply during the Late Quaternary. The width of the continental shelf also varies significantly, from a maximum of 20–25 km in the southern Bay of Salerno to 0.5–4 km in the northern part of the Bay, off the Amalfi coast, and the shelf break is typically located at a water depth of *c.* 120 m (Fig. 4). Here the continental shelf is dominated by a thick prograding succession of Late Pleistocene age (Conforti 2003; Sacchi *et al.* 2004) that is truncated by a major erosional unconformity (ES). The latter is due to subaerial exposure during the sea-level fall and lowstand of the last glacial age and/or marine erosion associated with a transgressive landward shift of the fair-weather wave base during the rapid sea-level rise that accompanied the Holocene
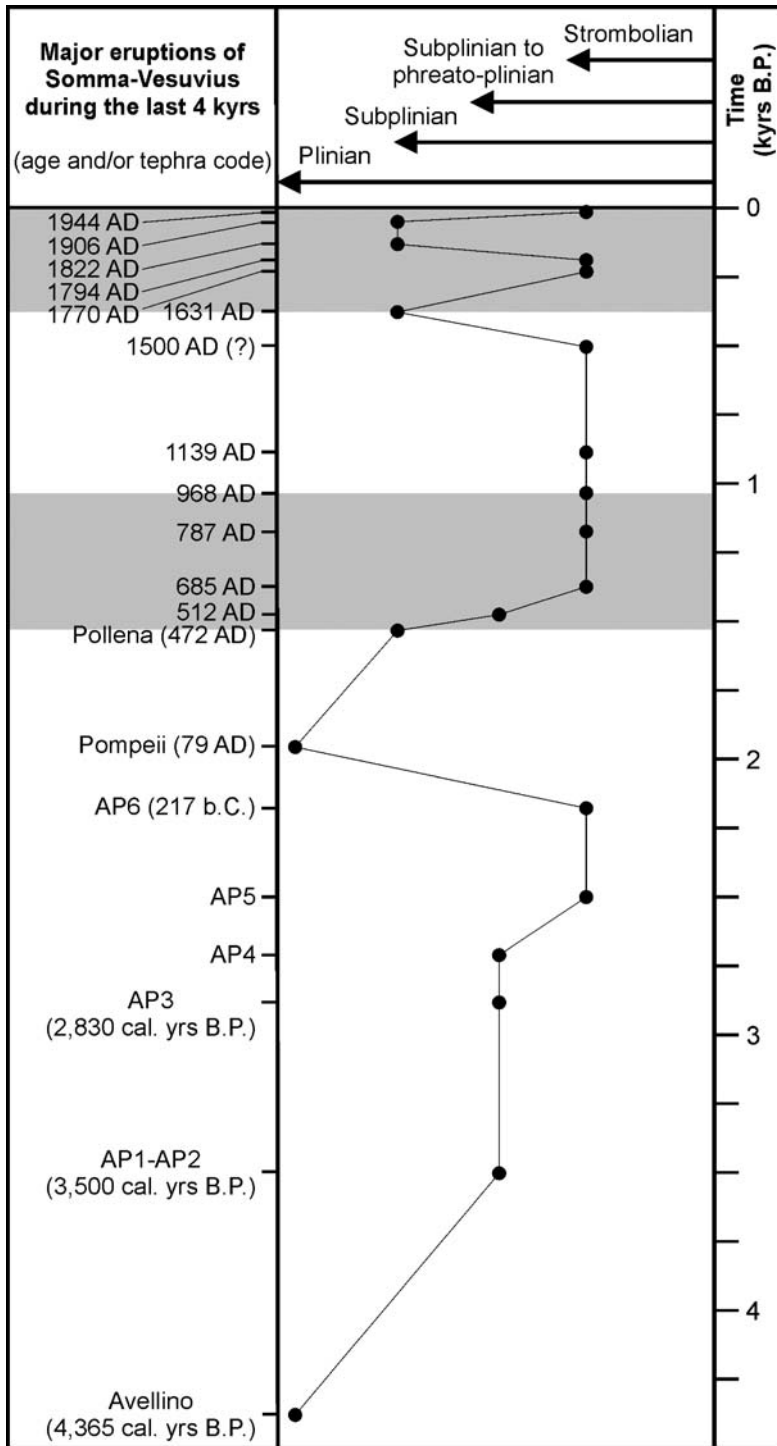
Fig. 3. List of the major eruptions of Somma–Vesuvius during the last 4000 years, with indication of the approximate explosive potential of events (after Santacroce *et al.* 2008). Time slices in grey are periods of semi-persistent volcanic activity.
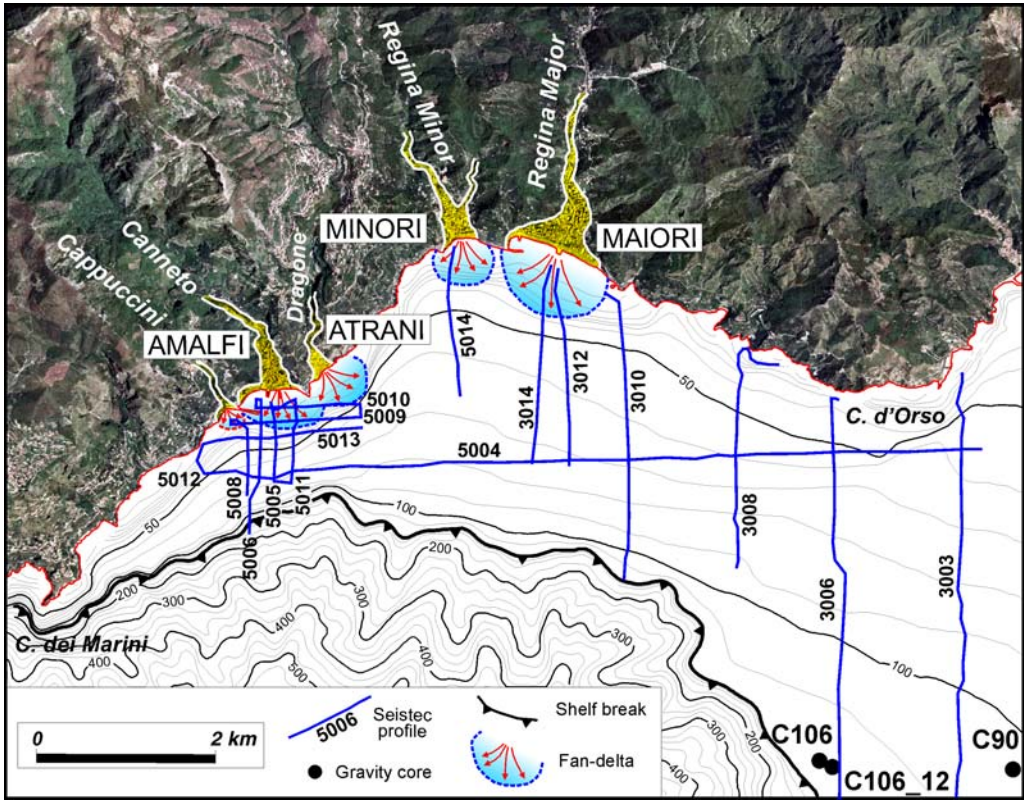
Fig. 4. Sketch-map of the alluvial fan-delta system of the Amalfi cliffed coast between Conca dei Marini and Capo d'Orso, with location of Seistec profiles and gravity cores illustrated in this study. (See Fig. 2 for location.)

deglaciation. The unconformity marks a stratigraphic gap ranging from a few thousand years to more than 70 ka. The maximum thickness of the post-glacial succession of the continental shelf in the northern Bay of Salerno may exceed 40 m.

Material and methods

This study is based on a very high-resolution (IKB-Seistec), single-channel reflection seismic survey carried out on the Amalfi inner shelf, between Salerno and Amalfi, in July 2004 (Fig. 4). The overall control for the stratigraphy and depositional setting of the late Quaternary depositional sequence comes from an extended dataset that includes multibeam bathymetry, side-scan sonar imagery, single-channel sparker and chirp-sonar profiles, sediment cores, and integrated biostratigraphic and chronological data acquired by the IAMC-CNR between 1997 and 2004. The sequence stratigraphic nomenclature adopted for seismic interpretation is after Hunt & Tucker (1992).

Seismic data acquisition

The seismic data presented in this paper include a grid of more than 100 km of very high-resolution single channel (uniboom) reflection profiles acquired using the IKB-Seistec profiler. This profiler has been designed specifically for collecting very high-resolution data in shallow-water environments but can also be used in water depths >200 m (Simpkin & Davis 1993; Mosher & Simpkin 1999). The Seistec system comprises a 2.5 m long catamaran supporting both the boomer source and receiver. The source is an IKB model B3 wide-band electrodynamic 'boomer' producing a single positive peak pressure impulse with a primary pulse width of 120 μs. The receiving system is a line-in-cone receiver located adjacent to the boomer plate (70 cm). The source emits useful frequencies in the range 1–20 kHz and, because of this wide frequency band, allows resolution of reflectors spaced 20 cm apart. Penetration is up to 100 m in soft sediments, and 200 m in deep-water soft sediments. During the survey, on board a

small boat at a speed of about 3 knots, a STEP power supply was used with a power of 150 J and a shot rate of 4–6 shots per second. Seismic data were recorded with a PreSeis digital acquisition system with 16 bits per sample, a sampling frequency of 100 kHz and a recording length of 60–100 ms. The position during navigation was determined by a differential global positioning system (GPS) directly mounted at the common depth point (CDP) of the IKB-Seistec profiler.

The exceptional time resolution and the fixed source–receiver geometry of the Seistec profiling system, together with its high sub-bottom penetration, allow for a quantitative analysis of the different seismic-signature shapes and geometries and signal amplitudes.

Gravity coring and laboratory analysis

Ground truthing of seismic records was provided by the detailed analysis of three gravity-cores (C90, C106, C106_12) collected on the outer shelf off the Amalfi coast (Fig. 4), as well as by the general description of a number of supplementary cores recovered from the mid–outer shelf of the northern Bay of Salerno. Sedimentological analysis included the recognition of major lithofacies associations, sedimentary structures, and grain-size analysis of selected stratigraphic intervals by laser diffractometry. The grade of bioturbation was estimated according to Droser & Bottjer (1991). Textural analysis of cores C90 and C106_12 was conducted at an average sampling rate of 3 cm, throughout the entire core length. Denser sampling was conducted for detailed study of transitional zones between different lithologies and/or sedimentary structures. Grain-size statistical parameters have been calculated following the classic graphical equations developed by Folk & Ward (1957).

Quantitative micropalaeontological analysis was conducted on 3 cm thick samples spaced every 10 cm. A minimum count of 100 specimens of benthic foraminifers for each sample was observed following the methods described by Fatela & Taborda (2002). The generic identification of foraminifers was made following Loeblich & Tappan (1988) and Sgarrella & Moncharmont-Zei (1993).

The carbonate content was measured on 10 g dry sediment samples, spaced every 10 cm. Mollusc fragments that could affect $CaCO_3$ analyses were handpicked and removed. Therefore, variations in carbonate content of the samples through the core record the occurrence of calcareous microfossils, in particular foraminifers and ostracodes, and nannofossils.

^{14}C accelerating mass spectrometry (AMS) measurements were performed with a system based on a tandem accelerator (9SDH-2, National Electrostatics Corporation) with a maximum terminal voltage of 3 MV. The $\delta^{13}C$ of each sample was also measured using an elemental analyser (ThermoFinnigan EA 1112) coupled with an IR mass spectrometer (ThermoFinnigan Deltaplus). Samples were pre-treated in accordance with the procedures outlined by Hoefs (1987), Vogel et al. (1984) and Passariello et al. (2007). Radiocarbon ages were calibrated by using the CALPAL-2007 software (Weninger & Jöris 2008; Weninger et al. 2008).

Data and results

Gravity-core stratigraphy

Gravity-cores C90, C106, C106_12 were collected on the outer shelf of the Bay of Salerno, between Capo d'Orso and Amalfi, at water depths of 103–116 m and provide a calibration of the entire postglacial succession. The length of recovered core sections ranges from 485 cm in cores C90 and C106 to 687 cm in core C106_12 (Figs 5 and 6).

Stratigraphic correlation of the gravity-cores is clear from the sedimentological analysis, thus allowing the construction of a composite stratigraphic section that represented the basis for the geological calibration adopted in the seismic stratigraphic interpretation. The cored succession consists of a c. 5 m thick transgressive sequence that overlies the major erosional surface (ES) associated with the sea-level fall and lowstand of the last glacial maximum. Below this unconformity, core C106_12 sampled a sandy silt succession older than 50 ka, within Upper Pleistocene deposits (Fig. 6).

The entire cored sequence is punctuated by at least 10 tephras, which we labelled from top to bottom as tS1, tS1-α, tS1-β, tS1-γ, tS2, tS2-α, tS3, tS3-α and tS4 to tS6. Of these, tS1–tS4 are interbedded within the post-glacial succession, whereas tS5 and tS6 are interbedded within the Upper Pleistocene deposits underlying unconformity ES. The tephra layers typically are several centimetres to a few decimetres thick. Most of them have a sharp base, normal or inverse grading, poor sorting and typically a gradual transition to the overlying deposits. An exceptionally thick tephra is represented by the 80–100 cm thick pyroclastic bed deposited during the AD 79 Plinian eruption of Vesuvius (tephra tS2; Sacchi et al. 2005; Insinga et al. 2008).

On the basis of sedimentological analysis and quantitative changes in benthic foraminiferal assemblages of the core samples, three main lithofacies associations can be recognized (Figs 7 and 8). A composite stratigraphic section, from bottom to top, consists of: facies A, shelf mud with volcaniclasts
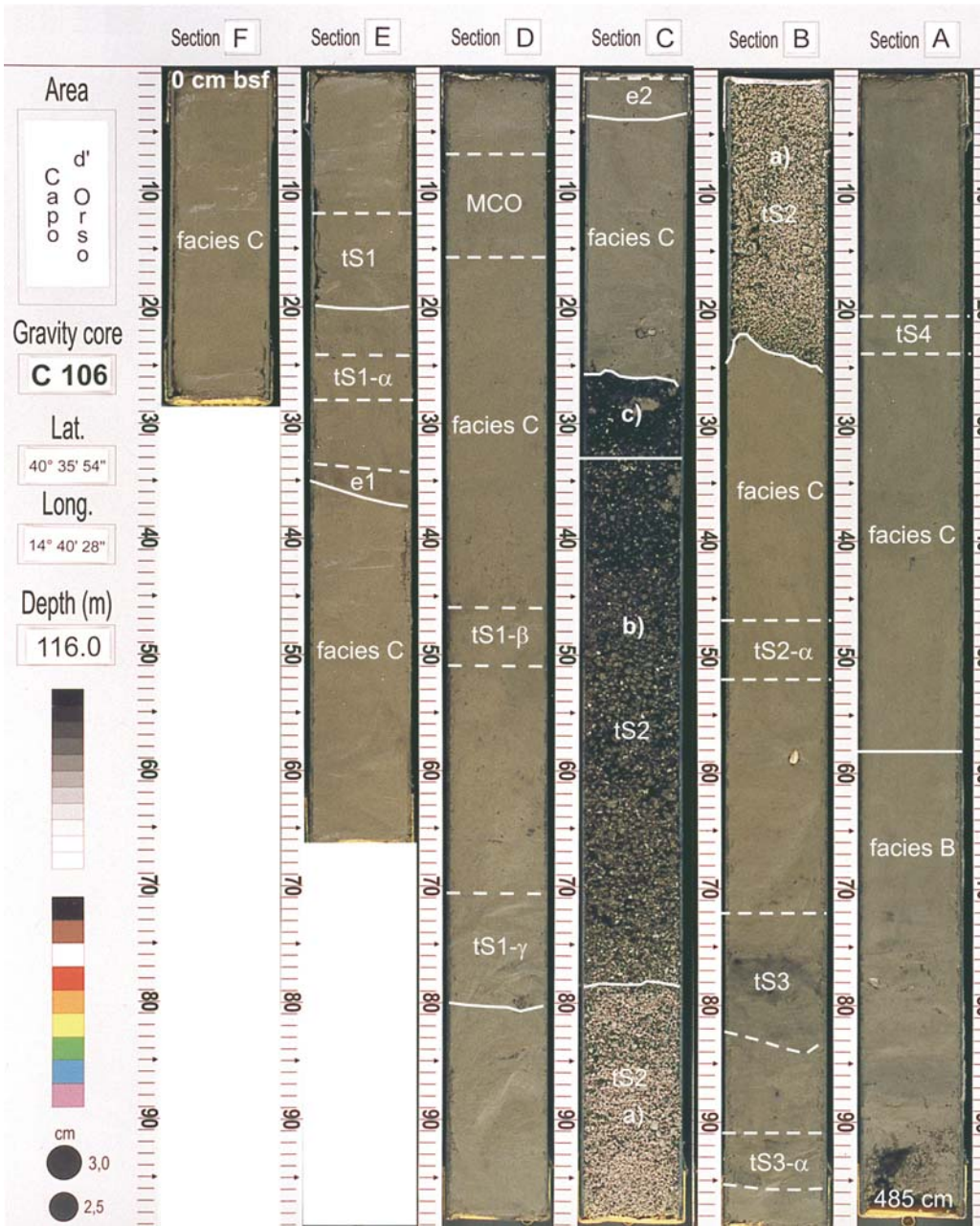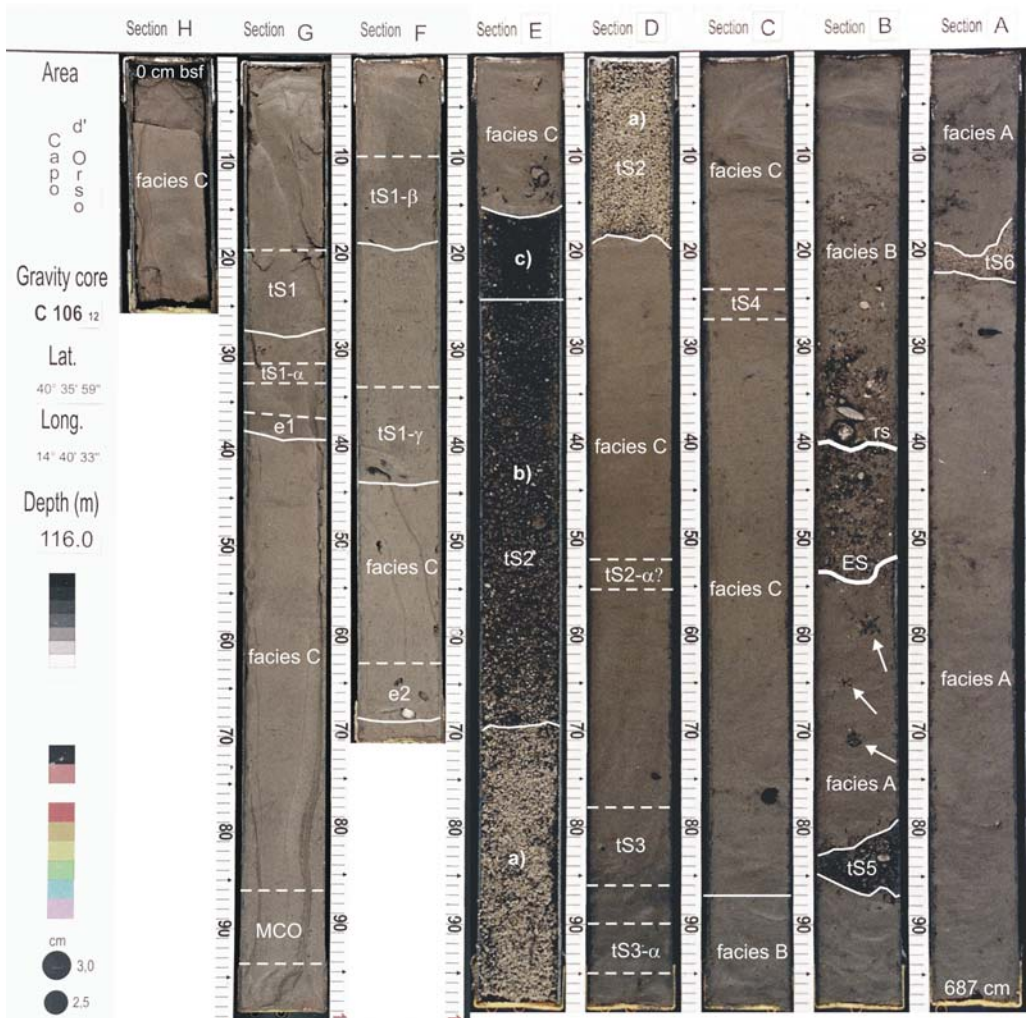
Fig. 5. Photograph of C106 core splits. Labels F to A denote core sections from top (0 cm bsf) to bottom (485 cm bsf). Total length of the core is 485 cm. MCO, Medieval Climatic Optimum; e1, suspension plume deposit; facies B, shoreface sand and pebble; facies C, bioturbated prodelta mud. Tephra layers (tSn) are also indicated. Key to sub-units of tS2 ('Pompeii', AD 79) fallout deposits: (a) white pumice; (b) grey pumice; (c) fine-grained lapilli. (For this and following figures, see Tables 1–3 for further information on chronology and nature of event beds.)

Gravity core C 106_12 (116 m bsl)

Fig. 6. Photograph of C106_12 core splits. Labels H to A denote core sections from top (0 cm bsf) to bottom (687 cm bsf). Total length of the core is 687 cm. Abbreviations as in Figure 5 and: ES, base of post-glacial succession; rs, ravinement surface; facies A, shelf mud with volcaniclasts and bioclasts. Arrows indicate *Thalassinoides* burrows (*Glossifungites* ichnofacies).

and bioclasts; facies B, shoreface sand and pebbles; facies C, bioturbated prodelta mud.

Facies A, shelf mud with volcaniclasts and bioclasts

This facies is represented only in core C106_12 and has a thickness of *c.* 110 cm. From base to top, it consists of poorly sorted olive grey (5Y4/2) clayey sandy silt and dark grey (5Y4/1) sandy

clayey silt interbedded with very thin volcaniclastic lenses. At 612 cm and 580 cm below sea floor (bsf) two pyroclastic layers occur: a 4 cm thick tephra (tS6) and a 9 cm thick tephra (tS5). The sandy fraction is represented by volcaniclasts and bioclasts and displays a gradual increase, especially in the volcaniclastic component, towards the top (Figs 6 and 7).

The benthic foraminiferal assemblage is mainly dominated by *Uvigerina peregrina*, *Cassidulina laevigata carinata*, *Hyalinea baltica*, *Melonis*
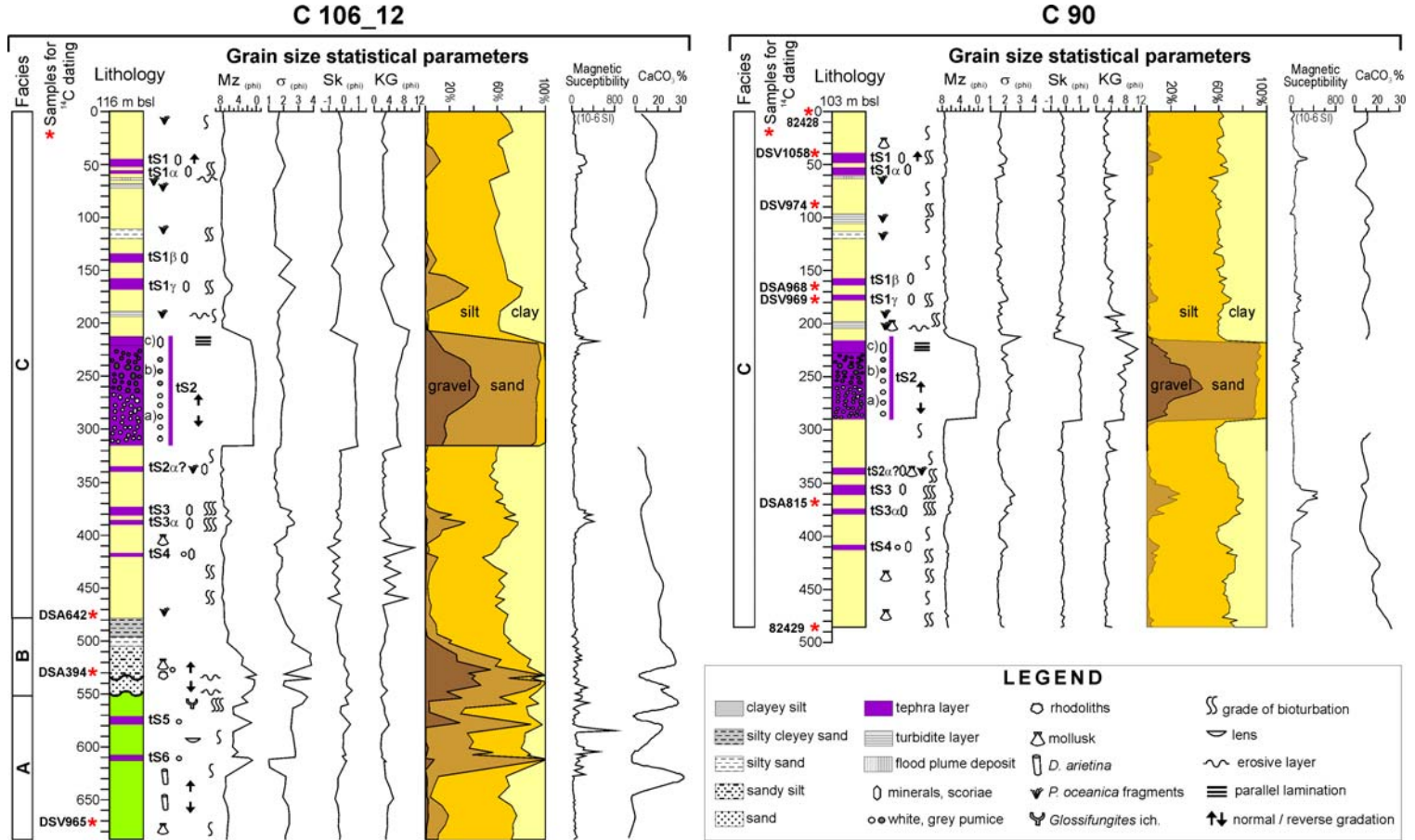
Fig. 7. Lithology, textures, sedimentary structures, magnetic susceptibility, calcium carbonate content and facies associations of gravity cores C90 and C106_12. Grain-size statistical parameters (Folk & Ward 1957): Mz, mean; σ, sorting; Sk, skewness; KG, kurtosis. Facies and tephra units as in Figure 5.
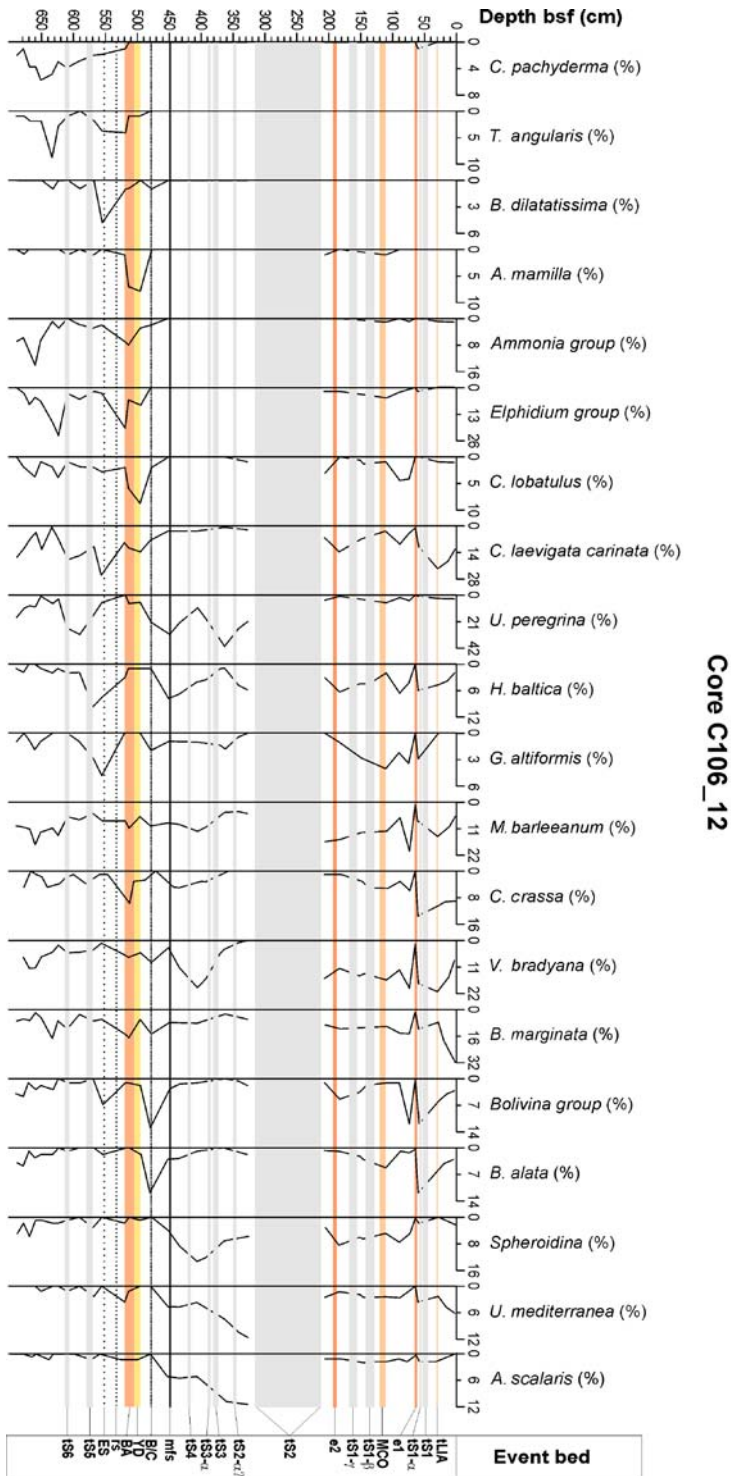
Fig. 8. Relative frequency (%) of selected benthic foraminifers and event beds of core C106_12.

barleeanum and *B. marginata*. These forms tend to increase in number towards the top of the unit, where they occur associated with rare *Valvulineria bradyana*, and the *Elphidium* and *Ammonia* groups. This association is typical of the lower circalittoral zone (e.g. Sgarrella & Barra 1984; Sgarrella & Moncharmont-Zei 1993). Specimens of broken pteropods are found (*Limacina retroversa*, *L. inflata* and *Clio pyramidata*). Fragments of polychaetes (*Ditrupa arietina*), bivalves, gastropods, bryozoans and echinoderms are present at 670 and 620 cm.

The occurrence in the foraminiferal assemblages of species typical of cold and productive waters, such as *C. laevigata carinata*, *Trifarina angulosa* and *H. baltica* (Murray 1991; Asioli 1996), of the *Elphidium* and *Ammonia* groups, as well as of *M. barleeanum* and *B. marginata*, coupled with the presence of *D. arietina*, suggests cold waters and stagnation episodes, possibly related to fresh-water runoff and relatively high concentration of fine-grained sediments and organic matter (Jorissen 1988; Grémare *et al.* 1998). The occurrence of the epipelagic boreal guest *Limacina retroversa*, from the northern cold-water regions, at present absent in the Mediterranean, suggests a cold period of the glacial Pleistocene (Buccheri 1984; Buccheri *et al.* 2002; Fig. 8).

The uppermost 20 cm of this unit show sparsely branching burrows of ichnogenus *Thalassinoides*. The burrows have well-defined circular boundaries, with diameter ranging from 1 to 2 cm, and are passively infilled with lithofacies B. This ichnofabric corresponds to the *Glossifungites* ichnofacies (Frey & Seilacher 1980; Pemberton & Frey 1985; MacEachern *et al.* 1992; Gingras *et al.* 2001; see Fig. 6). The unit is bounded at the top by an erosional surface that correlates with the unconformity ES of seismic profiles, and is characterized by the occurrence of shell debris. *Glossifungites* ichnofabric is commonly taken to indicate a firmground (see Gingras *et al.* 2001, and references therein). In this context it probably represents colonization of the Pleistocene eroded substrate during minor breaks in sedimentation following storm events, below storm wave base in the foreshore–offshore transition zone, during the early transgressive systems tract (TST). The lithofacies assemblage of this succession, coupled with the seismic evidence of thick Upper Pleistocene forestepping parase-quences beneath unconformity ES, suggests that this unit may be interpreted as a progradational deltaic sequence characterized by shelf mud deposit with volcaniclasts and bioclasts.

Facies B, shoreface sand and pebble

These deposits directly overlies facies A and consist of a 70 cm thick unit in core C106_12, whereas they represent the lowermost 40 cm of succession sampled at the C106 core site (Figs 5–7). The grain sizes of this unit range from silty sand to pebble, with very poor sorting. The lowermost 10 cm are represented by a medium sandy pebble sequence with inverse gradation that is bounded at the top by an erosive surface that correlates with the ravinement surface recognized on seismic pro-files. Towards its top, the deposit is characterized by coarse-grained constituents represented by volcaniclasts, lithoclasts and bioclasts, often frag-mented. The matrix is formed by the same constit-uents. Lithoclasts are rounded, often reddened, and include carbonate rock fragments (calcilutite) at places encrusted by red coralline algae (rhodoliths). Volcaniclasts are sub-rounded to sub-angular, locally reddened, and consist of light grey and green pumice, mineral grains (mostly sanidine, pyr-oxene and rare magnetite crystals) that are often rounded and abraded, scoriae and glass. The bio-clasts include bivalve and gastropod shell frag-ments, which are sometimes abraded, bioeroded and encrusted, solitary corals, bryozoans and echi-noid fragments. Plant debris (*Posidonia oceanica*) is also found (Fig. 7).

In the lower part of this unit, the benthic assem-blage is represented by the *Elphidium* group, *B. marginata*, *C. laevigata carinata*, *M. barleeanum* and the *Ammonia* group, which are partly replaced towards the top by epiphytic species typical of det-rital sediments (*Cibicides lobatulus*, *Asterigerinata mamilla*, *Planorbulina mediterranensis*) (Jorissen 1987; Sgarrella & Moncharmont-Zei 1993; Fig. 8). The occurrence of *C. laevigata carinata* and *M. bar-leeanum* in the benthic assemblage at the bottom of the unit may indicate an increased delivery of organic matter but minor oxygen depletion (Caralp 1988; Asioli *et al.* 2001). The benthic assemblage at the top of the interval indicates that water depth is somewhat shallower than for the underlying facies A, and the occurrence of *C. laevigata carinata* suggests cold and productive waters (e.g. Asioli 1996). The *Elphidium* group and *C. lobatulus* toler-ate hyposaline conditions and may resist severe sal-inity fluctuations (Murray 1973, 1976; Boltovskoy 1976). These observations, along with the occur-rence of rhodolith-bearing pebbles and shells, indi-cate a infralittoral to circalittoral zone associated with relatively low-salinity conditions. On the basis of lithofacies assemblages and the seismic-stratigraphic architecture, this unit can be inter-preted as a transgressive lag containing reworked material from the substrate and/or the early shore-face deposits ('healing phase deposits') (e.g. Posamentier & Allen 1993).

A negative peak of the $CaCO_3$ curve in the inter-val between 495 and 505 cm (C106_12), which suggests a relatively low water temperature, may be

tentatively correlated with the Younger Dryas (Kallel *et al.* 1997). Analogously, the underlying interval between 505 and 525 cm (C106_12), marked by a positive peak of the $CaCO_3$, may be taken as corresponding to the Bölling–Allerød event (Fig. 7).

Facies C, bioturbated prodelta mud

Facies C is represented in all the study cores and has a thickness of 212 cm (C106_12) to 118 cm (C90 and C106). It consists of a mud-supported lithofacies characterized by a grey to olive grey homogeneous, bioturbated clayey silt with at least eight tephra (or cryptothepra) interbedded with a few thin layers of fine-grained turbidites (Figs 5–7).

The sandy fraction is rare and consists of fine to very fine volcaniclasts, sub-rounded to sub-angular grey pumice, mineral grains, scoriae and glass, and bioclasts (represented by fragments of gastropods, bivalves, bryozoans and echinoids) and very rare fragments of pteropods (*C. pyramidata, Creises*

sp., *L. inflata*). Turbidite layers are a few centimetres thick and consist of volcaniclasts (rounded pumice, locally reddened scoriae, fragments of minerals), sub-rounded lithic fragments and reworked bioclasts (fragments of bivalves, gastropods, bryozoans, phanerogamous seagrass remains) (Fig. 7).

In the upper part of the succession, a few centimetres below tephra ts1-α, a 2–3 cm thick layer of grey homogeneous bioturbated clayey silt, characterized by an extremely reduced faunal content and rare *Posidonia oceanica* fragments, occurs (layer e1 in Figs 5–8). This layer can be correlated across all the study cores and may be interpreted as a suspension plume deposit (Nemec 1995; Parsons *et al.* 2001), probably associated with the exceptional flood events that affected the Amalfi coast in 1581 and 1588 (Figs 8–11; Porfido *et al.* 2009).

Facies C marks a significant change in the relative abundance of many benthic taxa, accompanied by the disappearance and/or abrupt decrease of
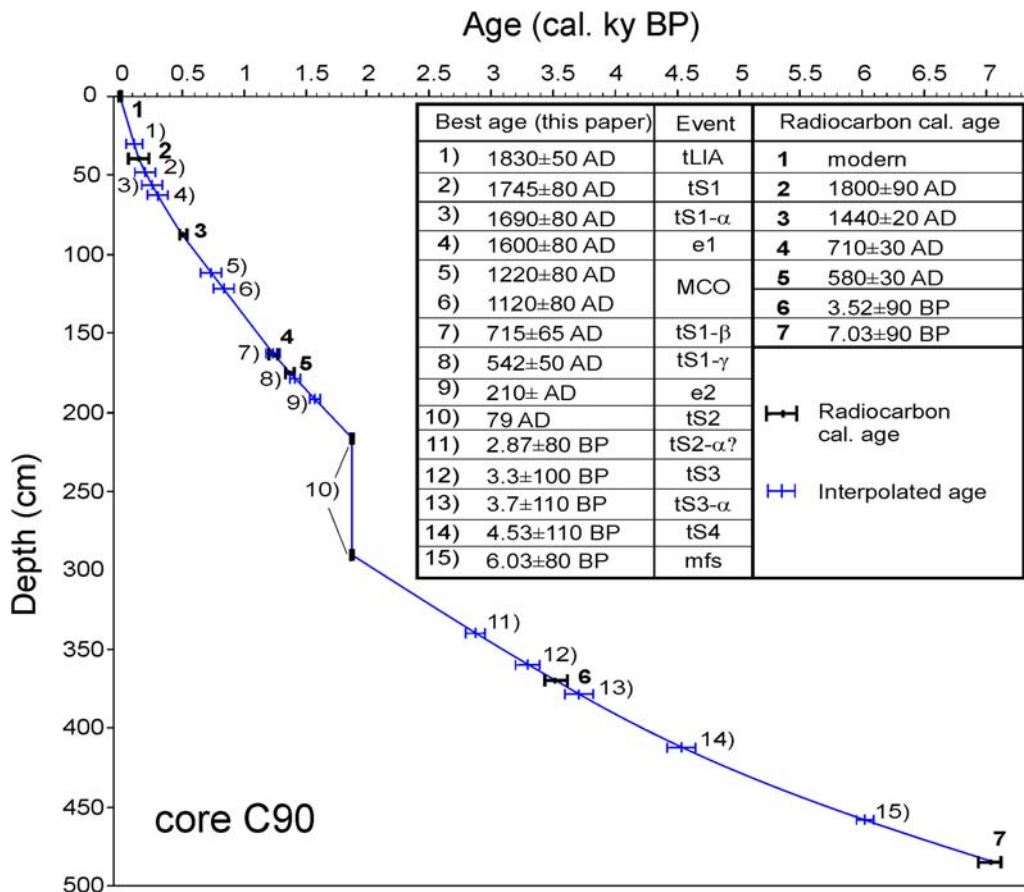

Fig. 9. Age–depth model of gravity core C90 based on calibrated AMS ^{14}C data and tied to the age of the tephra bed deposited by Vesuvius during the Plinian eruption of Pompeii (AD 79).
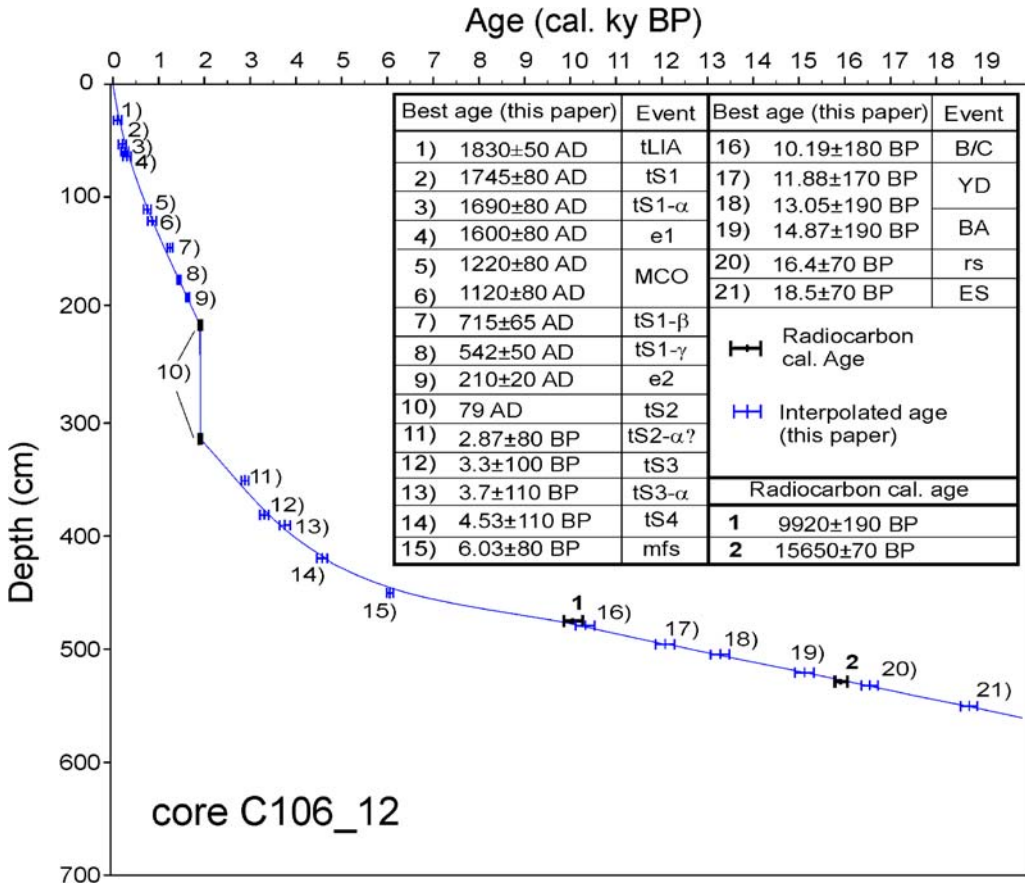
Fig. 10. Age–depth model of gravity core C106_12 based on calibrated AMS ^{14}C data and tied to the tephra bed deposited by Vesuvius during the Plinian eruption of Pompeii (AD 79).

some species (*Cibicidoides pachyderma*, *T. angulosa*, *Bolivina dilatatissima*, *Ammonia* group) and the parallel increase of others (e.g. *U. peregrina*, *U. mediterranea*, *Amphycorina scalaris*, *M. barleeanum*, *B. marginata*, *H. baltica*). Peaks of maximum abundance of some taxa, along with a relative maximum in the CaCO$_3$ curve, seem to concentrate around 450 cm, at a stratigraphic horizon we interpret as the maximum flooding surface (mfs) (Figs 7 and 8).

The AD 79 Pompeii tephra bed (tS2) corresponds to a marked environmental change in the faunistic assemblage (Fig. 8). Some taxa associated with the shallow infaunal microhabitat (*U. peregrina*, *U. mediterranea*, *H. baltica*, *Gyroidina* sp.) that had proliferated at the top of facies B, display, after tephra tS2, a sudden decrease in relative abundance, whereas opportunistic species (*V. bradyana*), intermediate infaunal (*M. barleeanum*) and deep infaunal species (*B. marginata*) that could probably better survive the increased sedimentation rates

are recorded particularly after this event (Jorissen 1987; Linke & Lutze 1993; Jorissen & Wittling 1999; Schmiedl *et al.* 2000). Further upward the gradual decrease in abundance of taxa typical of cold and productive waters (*C. laevigata carinata*, *H. baltica*) (Murray 1991; Asioli 1996) probably indicates a relative maximum in the warming of bottom waters and culminates in a period that can be correlated with the Medieval Climatic Optimum (MCO). At 30 cm bsf the same species display a relative increase and are associated with opportunistic species (*V. bradyana*, *M. barleeanum*), thus suggesting relatively cooler waters and possibly increased freshwater input (Asioli 1996). According to our results this event has a probable age of AD 1830 $\pm/-50$ and may be tentatively correlated with the termination of the Little Ice Age (tLIA) (Figs 8–10).

In general, the benthic assemblage of this unit indicates a rapid increase in sedimentation rate relative to the underlying facies B and a predominantly
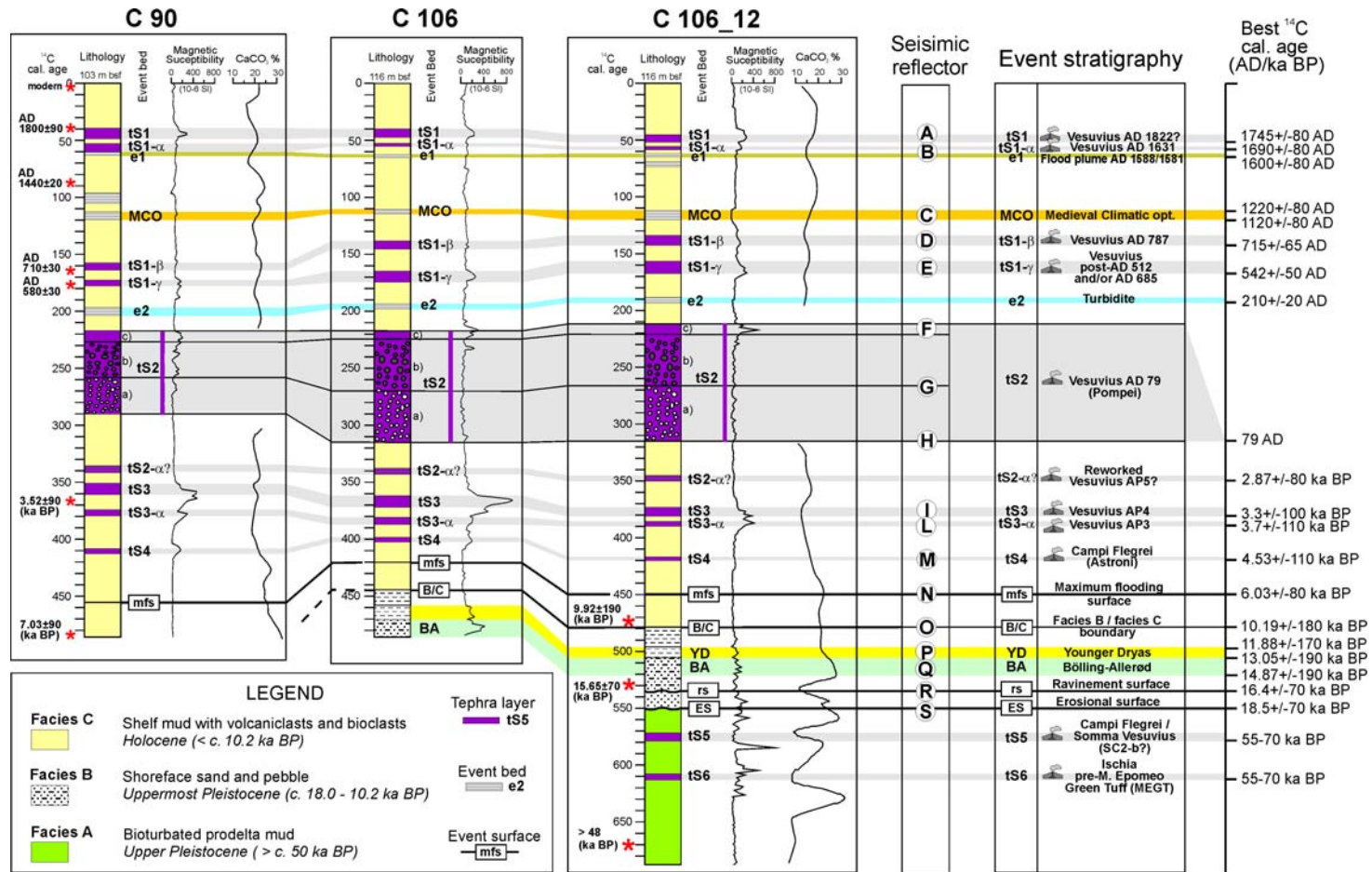
Fig. 11. Correlation of gravity cores used in this study and interpolated ^{14}C chronology of major tephra layers and other event beds. Key to sub-units of tS2 as in Figure 5.

muddy setting, characterized by relatively high organic matter and low oxygen concentration, typical of the modern 'mud belt' (Jorissen 1988). Correlation with seismic profiles suggests that this lithofacies corresponds to prodelta mud deposits associated with the modern fan-delta system of the Amalfi shelf.

^{14}C chronology and tephra layers

The AMS radiocarbon ages obtained from sampled marine material are reported in Table 1. The calibrated ages obtained are in a general agreement with the stratigraphic position of the samples and provide an absolute age constraint for the last *c.* 16 ka BP as well as a potential cross-check for chronological attribution of tephra layers. A modern age (i.e. AD 1950) resulted from the top of core C90 (sample 82428), whereas age determination for sample DSV965 was not possible as it was outside the scale of the adopted AMS system (i.e. >48 ka BP). The ^{14}C calibrated age models obtained for cores C90 and C106_12 are illustrated in Figures 9 and 10. According to the ^{14}C calibrated age–depth plots we obtain interpolated ages that provide a chronological reference for the recognized event beds and can be used for tentative correlation of the studied tephra layers with age-dated volcanic events onland. Correlation between the study cores is illustrated in Figure 11. The preferred ages and proposed interpretation of tephra layers and other event beds are reported in Tables 2 and 3.

Tephras tS1, tS2, tS3 and tS3-α have been recently described by Insinga *et al.* (2008). These pyroclastic layers have been interpreted, on the basis of stratigraphic and chemical analysis, as the products of the Vesuvian activity of the last 3 kyrs and have been correlated with the eruptions of AD 1822 or 1631 (tS1), the eruption of AD 79 (tS2), and the inter-Plinian events (tS3-α and tS3) referred to in the literature as AP3 and AP4, respectively (Andronico & Cioni 2002). Interpolated ages allow us to include tephra tS1 and tS1-α in the time span AD 1825–1665 and 1770–1610, respectively. During these time intervals only the AD 1631 and 1822 events reached sub-Plinian intensity and only the AD 1779 and 1794 eruptions were accompanied by a phreatomagmatic phase. This evidence suggests a possible correlation of tephra tS1 with the 1822 event (Insinga *et al.* 2008, and references therein) and tephra tS1-α with the 1631 eruption (Rolandi *et al.* 1993; Rosi *et al.* 1993). Sedimentological analysis, however, indicates that an eventual amalgamation of more tephra layers deposited by different eruptions occurring during the semi-persistent activity of the Vesuvius that followed the AD 1631 event cannot be excluded.

Table 1. *Summary of the AMS ^{14}C results on sediment core samples from the Bay of Salerno*

Core	Lab. code	Sample number	Depth bsf (cm)	Material	^{14}C age (years BP)	$\delta^{13}C$	$\Delta(\delta^{13}C)$	Cal. age (years BP)
C90	LLL	82428	0–3	Planktonic foraminifers	Modern	–	–	Modern
C90	CIRCE	DSV1058	39	Shell	484 ± 21	2.95	0.42	AD 1800 ± 90
C90	CIRCE	DSV974	87	Marine plant remains	826 ± 25	−24.49	1.19	AD 1440 ± 20
C90	CIRCE	DSA968	164	Shell	1680 ± 20	1.06	0.22	AD 710 ± 40
C90	CIRCE	DSV969	175	Bryozoan	1872 ± 25	6.82	0.63	AD 580 ± 30
C90	CIRCE	DSA815	370	Shell	3678 ± 84	3.24	1.16	3520 ± 90 years BP
C90	LLL	82429	480–485	Planktonic foraminifers	6515 ± 45	–	–	7030 ± 90 years BP
C106_12	CIRCE	DSA642	475	Shell	9239 ± 106	7.80	1.78	9920 ± 190 years BP
C106_12	CIRCE	DSA394	529	Shell	13 676 ± 45	5.33	0.49	15 650 ± 70 years BP
C106_12	CIRCE	DSV965	672	Shell	>48 ka	−10.25	0.48	>48 ka

LLL, Lawrence Livermore Laboratory, CA, USA; CIRCE, Centre for Isotopic Research for Cultural and Environmental Heritage, Caserta, Italy.

Table 2. *Interpolated ages of post-glacial event beds at C90 and C106_12 core sites, according to the ^{14}C cal. age model presented in this study (Figs 9 and 10)*

Bed code	Nature of event	Gravity core	Depth to base (cm)	Depth to top (cm)	Thickness (cm)	Correlative sesimic reflector	^{14}C cal. age
tS1	Tephra layer	C90	48	39	9	A (top + bottom)	AD 1745 ± 80
		C106_12	53	45	8		
tS1-α	Tephra layer	C90	60	53	7	B (top + bottom)	AD 1690 ± 80
		C106_12	59	57	2		
e1	Flood plume deposit AD 1588–1581	C90	63	60	3		AD 1600 ± 80
		C106_12	65	63	2		
MCO	Medieval Climatic Optimum	C106_12	120	113	7	C (top + bottom)	AD 1220 ± 80 to 1120 ± 80
		C106_12	120	111	9		
tS1-β	Tephra layer	C90	163	157	6	D (top + bottom)	AD 715 ± 65
		C106_12	143	134	9		
tS1-γ	Tephra layer	C90	178	172	6	E (top + bottom)	AD 542 ± 50
		C106_12	168	158	10		
e2	Turbidite layer	C90	204	197	7	–	AD 210 ± 20
		C106_12	194	187	7		
tS2	'Pompeii' pumice fall AD 79	C90	290	217	73	F (top) G (white–grey pumice boundary) H (bottom)	AD 79
		C106_12	314	213	101		
tS2-α?	Reworked tephra layer	C90	342	336	6	–	2.87 ± 80 ka BP
		C106_12	350	345	5		
tS3	Tephra layer	C90	361	351	10	I (top + bottom)	3.3 ± 100 ka BP
		C106_12	381	373	8		
tS3α	Tephra layer	C90	379	375	4	L (top + bottom)	3.7 ± 110 ka BP
		C106_12	390	385	5		
tS4	Tephra layer	C90	412	408	4	M (top + bottom)	4.53 ± 110 ka BP
		C106_12	420	417	3		
mfs	Maximum flooding surface	C90	455	–	–	N	6030 ± 80 ka BP
		C106_12	450	–	–		
B/C	Facies B–C boundary	C106_12	479	–	–	O	10.19 ± 180 ka BP
YD	Younger Dryas	C106_12	505	497	8	P (top + bottom)	11.88 ± 170 to 13.05 ± 190 ka BP
BA	Bölling–Allerød	C106_12	521	505	16	Q (top + bottom)	13.05 ± 190 to 14.87 ± 190 ka BP
rs	Ravinement surface	C106_12	531	–	–	R	16.4 ± 70 ka BP
ES	Erosional surface	C106_12	550	–	–	–	18.5 ± 70 ka BP

See also Figures 11 and 13 for further detail on correlation between event beds and seismic reflectors.

Table 3. *Marine tephra layers described in this study and proposed correlation with proximal pyroclastic deposits documented onland*

Tephra code	Lithology and texture of marine tephra	Suggested correlation with proximal tephra (age expressed as ^{14}C cal. years BP)	References
tS1	Fine- to very fine-grained dark grey ash (5y3/2) with clayey matrix. Ash made of leucite-bearing scoria (mostly analcimized), scarce pumiceous glass shards, lithic fragments, loose crystals. Sharp base	AD 1822? (Vesuvius)	Arrighi *et al.* 2001 Budillon *et al.* 2005 Insinga *et al.* 2008
tS1-α	Fine- to very fine-grained dark grey ash (5y3/2) with clayey matrix. Ash made of scoria, abundant lithic fragments and very rare glass shards (pumiceous type), loose crystals (clinopyroxene and feldspar). Sharp base in core C106	AD 1631 (Vesuvius)	Rolandi *et al.* 1993 Rosi *et al.* 1993
tS1-β	Fine- to very fine-grained bioturbated ash dispersed in clayey matrix (cryptotephra). Ash made of brown pumiceous glass shards with tubular and ovoid vesicles, leucite-bearing lithic fragments, minor scoria and obsidian. Loose crystals (mostly K-feldspar, clinopyroxene and biotite)	AD 787 (Vesuvius)	Rolandi *et al.* 1998
tS1-γ	Fine- to medium-grained dark grey (5y3/2) ash made of dark and light grey, leucite-bearing scoria, pumiceous glass shards, leucite-bearing lithic fragments and loose crystals (K-feldspar, clinopyroxene and biotite). Sharp base	Post AD 512 activity and/or AD 685 (Somma–Vesuvius)	Rolandi *et al.* 1998 Iorio *et al.* 2004
tS2	Coarse- to fine-grained white phonolitic pumice lapilli overlain by coarse-grained grey tephriphonolitic pumice lapilli and coarse-grained dark grey ash. Scoria, carbonate lithic fragments and loose crystals are diffuse throughout the entire tephra. Sharp base and top	AD 79 ('Pompeii') (Somma–Vesuvius)	Sacchi *et al.* 2005 Insinga *et al.* 2008
tS3	Fine- to medium-grained dark grey (5y3/2) bioturbated ash in silty matrix. Ash made of leucite-bearing phonotephritic scoria and scarce pumice. Loose crystals (mostly K-feldspar and biotite)	AP4 (Somma–Vesuvius)	Rolandi *et al.* 1998 Andronico & Cioni 2002 Iorio *et al.* 2004 Insinga *et al.* 2008
tS3α	Fine- to medium-grained dark grey (5y3/2) bioturbated ash in silty matrix. Ash made of leucite-bearing phonotephritic scoria and scarce pumice. Loose crystas (mostly K-feldspar and biotite)	AP3 (Somma–Vesuvius) 2830 ± 50 years BP	Rolandi *et al.* 1998 Andronico & Cioni 2002 Iorio *et al.* 2004 Insinga *et al.* 2008
tS4	Fine- to very fine-grained ash dispersed in clayey silty matrix. Ash made mostly of loose K-feldspars, white pumice with tubular vesicles, glass shards, minor scoria and lithic fragments. Glass shards show blocky, platy, tubular and rare thick-walled morphologies. Loose crystals of clinopyroxene	Astroni (Campi Flegrei) 4244 ± 91 years BP	Di Vito *et al.* 1999
tS5	Coarse- to medium-grained ash made of reddish sub-angular, almost aphyric pumice with tubular and ovoidal vesicles, brown and yellow glass shards and dark grey scoria. Scarce lithic fragments. Glass shards show blocky, tubular and thin-walled bubble wall morphologies	SC2-b (?) (Campi Flegrei or Somma–Vesuvius) *c.* 55–65 ka BP	Di Vito *et al.* 2008
tS6	Coarse- to medium-grained white ash made of sub-angular, almost aphyric pumice, scarce blocky shards and lithic fragments. Loose crystals (mostly K-feldspar and pyroxene). Sharp base	pre-'M. Epomeo Green Tuff' events (Ischia) *c.* 55–65 ka BP	Vezzoli 1988 Brown *et al.* 2008 Di Vito *et al.* 2008

Cryptotephra tS1-β and tephra tS1-γ can be correlated with the Medieval activity of Vesuvius between the end of the fifth century and the eighth century. Their phonotephritic composition (unpublished data) suggests that they might be the product of the explosive activity that postdate the AD 512 eruption. Historical documents (Figliolo & Marturano 1994; Lirer *et al.* 2005) reported the AD 685 and 787 eruptions as the major events during this period. More recently, Cioni *et al.* (2008) described onland some ash layers referred to volcanic activity that took place soon after AD 512. According to these considerations we propose a possible correlation of tephra tS1-β with the AD 787 eruption, whereas tephra tS1-γ may represent the products of the activity that occurred after AD 512, including the AD 685 event. Tephra layers associated with this chronological interval occur as well-preserved marker horizons within the Upper Holocene succession and have been recently recognized offshore the Campania region (Insinga *et al.* 2008, and references therein) as well as in distal settings (i.e. Monticchio Lake, Wulf *et al.* 2008).

Tephra tS2 is a *c.* 1 m thick, distinctive pyroclastic bed formed by the air-fall deposits associated with the Plinian eruption of Vesuvius of AD 79 (Sigurdsson *et al.* 1985; Cioni *et al.* 1992; Sacchi *et al.* 2005). At the core C106_12 site, it consists of three major horizons represented from bottom to top by: (1) 48 cm thick, inversely graded, subrounded, white pumice and lapilli; (2) 44 cm thick, normally graded, sub-angular, coarse grey pumice lapilli and lithic fragments; (3) 9 cm thick, parallel-laminated coarse pumiceous and scoriaceous lapilli, including loose crystals (biotite and pyroxenes), abundant small mollusc fragments, carbonate lithoclasts, and other lithic fragments (see Fig. 6). The tephra bed corresponds to a pronounced seismic horizon that can be traced all across the Bay of Salerno (Sacchi *et al.* 2005).

Tephras tS3 and tS3-α have been correlated by Insinga *et al.* (2008) with the AP inter-Plinian activity (Andronico & Cioni 2002), on the basis of their lithological and chemical composition. In particular, these deposits have been interpreted as the products of the AP4 and AP3 (2830 ± 50 ^{14}C cal. years; Rolandi *et al.* 1998) events. The age–depth plots we have obtained here, however, point to significantly older ^{14}C interpolated ages, namely 3300 ± 100 years (cal. BP) for tephra tS3 and 3700 ± 110 years (cal. BP) for tephra tS3-α. On the basis of this interpretation, the volcaniclastic layer that lies above ts3 (ts2-α in Table 2) may be tentatively correlated with the younger AP eruptions (Andronico & Cioni 2002).

The interpolated ^{14}C age for tephra tS4 of 4350 ± 90 years BP, along with its homogeneous trachyphonolitic composition (unpublished data),

suggests a correlation of this deposit with the explosive Campi Flegrei events of Astroni dated at 4244 ± 91 ^{14}C cal. years BP (Di Vito *et al.* 1999). Products related to these eruptions have been reported elsewhere in the Bay of Naples (Insinga 2003) and more distal settings (Siani *et al.* 2004; Wulf *et al.* 2004).

Tephras tS5 and tS6 have been cored within the Upper Pleistocene deposits, beneath the unconformity ES (Figs 6 and 12–14) and are characterized by a trachytic and trachyphonolitic composition respectively (unpublished data). On the basis of the AMS radiocarbon data that indicate ages older than 48 ka BP, the expected ages of these tephras are between *c.* 60 ka and 80 ka BP. The attribution of tephra tS5 to a specific source is not an easy task because of the large number of volcanic events with similar geochemical signatures that occurred in the region between *c.* 44 ka and 75 ka BP (Pappalardo *et al.* 1999; Di Vito *et al.* 2008). However, the lithology and stratigraphic position of tephra tS5 suggests a correlation with the subaerial products of the activity of Somma–Vesuvius or Campi Flegrei between 55 and 70 ka BP (e.g. tephra SC2-b of Di Vito *et al.* (2008)). The very evolved trachyphonolitic composition of pumice suggests the island of Ischia as a possible source area for tephra tS6 (Insinga 2003). High-intensity explosive eruptions took place on the island during that time interval (Brown *et al.* 2008) and caused the widespread deposition of several tephra layers over the Campania Plain (Di Vito *et al.* 2008) and at more distal sites (Paterne *et al.* 1988; Wulf *et al.* 2004). In particular, tephra tS6 might be correlated with one of the several explosive events characterized by the deposition of pumice lapilli that predate the Monte Epomeo Green Tuff (MEGT) eruption (*c.* 55 ka BP; Vezzoli 1988), such as the Mago and/or Mt. S. Angelo eruptions (55–74 ka BP) described by Brown *et al.* (2008).

Core and seismic data correlation

Integrated stratigraphy and correlation of gravity-cores allowed for a bed-to-bed calibration of seismic reflectors. All the studied cores are located on the outer shelf, where the Holocene wedge is relatively thin and the typical range of penetration of standard gravity-cores ensured sampling of the entire post-glacial succession, down to the upper Pleistocene prograding units. In particular, core–seismic correlation for the entire Holocene section was established at C106_12 core site, located at *c.* 500 m from the southern edge of the track of Seistec profile 3006 (Figs 12 and 13). Depth (m) to time (ms) conversion of the C106_12 core log was calculated using an average velocity of seismic waves of *c.* 1600 m s^{-1} within the cored succession.
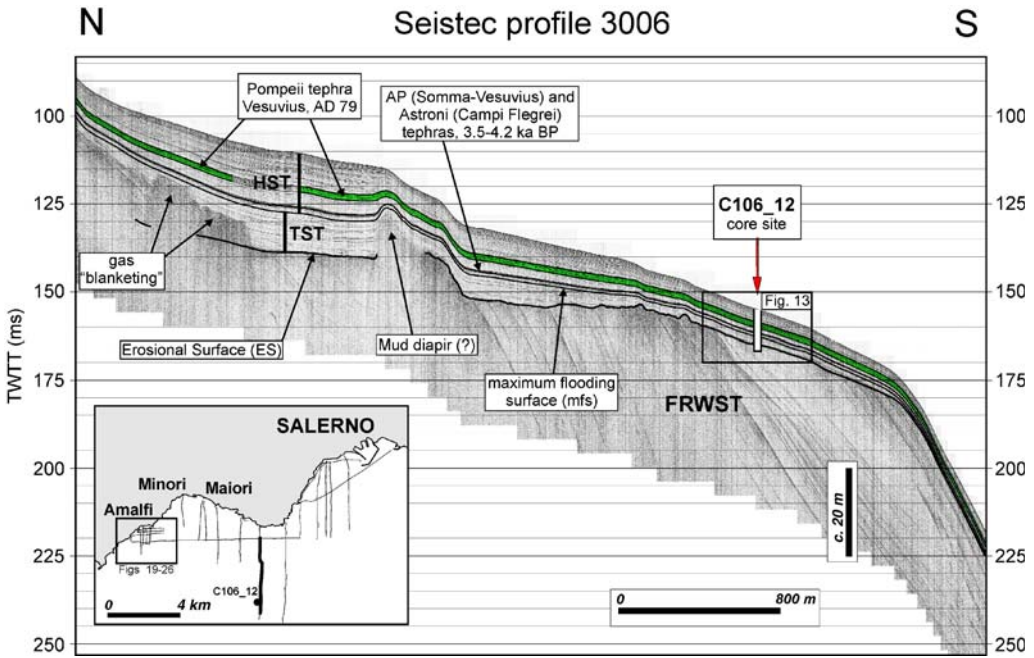
Fig. 12. Seistec profile 3006 showing the general architecture of the continental shelf off the Amalfi coast and the location of C106_12 core site. Erosional surface (ES) separates the Upper Pleistocene forced regression wedge prograding units (FRWST) from the above Uppermost Pleistocene–Holocene, post-glacial, transgressive systems tract (TST) and highstand systems tract (HST) deposits. TWTT, two-way travel time. Sequence stratigraphic nomenclature is after Hunt & Tucker (1992). Inset shows location of profile.
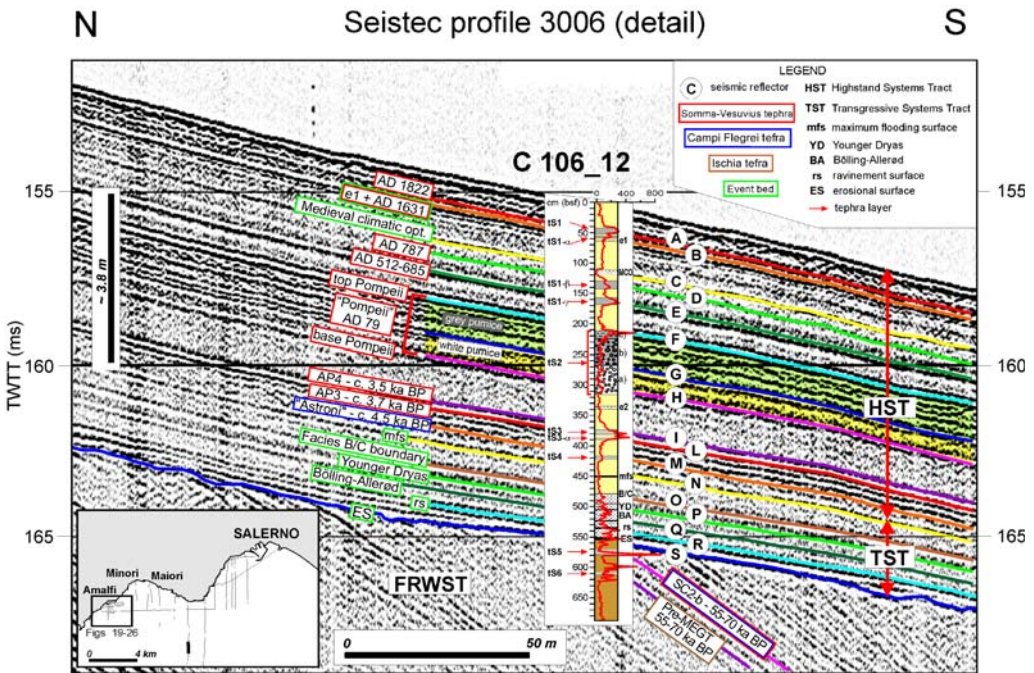
Fig. 13. Geological calibration and labelling of seismic reflectors of Seistec profile 3006 at C106_12 core site (see Fig. 12 and inset for location of profile). Key to sub-units of tS2 as in Figure 5.
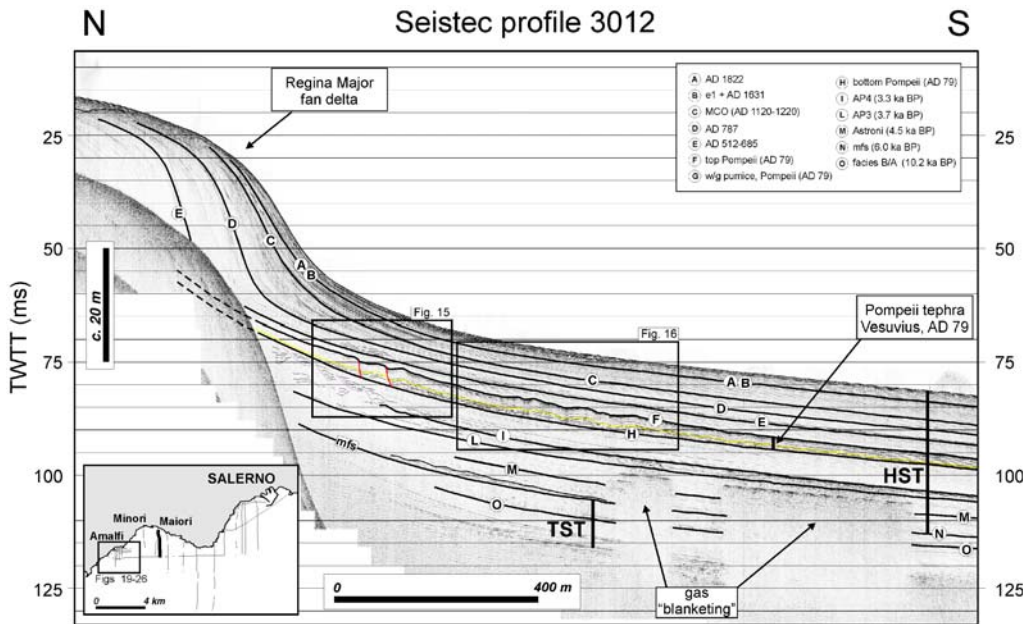
Fig. 14. Seistec profile 3012 offshore Maiori and its interpretation showing the fan-delta fed by the Regina Major stream and sedimentary structures associated with gravity-driven instability on delta slopes. Inset shows location of profile. Boxes indicate location of Figures 15 and 16.

Correction for sediment compaction was obtained by using the sea floor, tephra tS2 and unconformity ES as stratigraphic tie points (Fig. 13).

Core–seismic correlation allowed for calibration of the major sequence stratigraphic surfaces on seismic profiles (e.g. transgressive surface, ravinement surface, maximum flooding surface). Moreover, it indicates that tephra layers tend to correspond to high-amplitude, well-developed seismic reflectors. This is clearly the case, for instance, of the Vesuvius early Medieval tephra tS1-γ, the tS2 (AD 79) pumice fall layer, the tS3 and tS3-α (AP inter-Plinian deposits) and tephra tS4 (Astroni–Averno).

Seismic interpretation

The IKB–Seistec seismic profiles imaged the seafloor subsurface down to c. 60 ms two-way travel time (c. 100 m) beneath the sea floor. Maximum penetration of the seismic signal was recorded in the Capo d'Orso area, where the Upper Pleistocene prograding units can be thoroughly traced beneath unconformity ES (Figs 12 and 13). In the Amalfi area acoustic penetration was somewhat less, because of significant attenuation of seismic waves at depth or blanketing of the seismic signal by gas-saturated layers. Maximum vertical resolution is of the order of 20 cm.

Seistec profiles show that unconformity ES separates two main seismic stratigraphic units (Figs 12 and 13). The lower one is represented by a prograding succession truncated at the top by a dramatic erosional surface, and mostly consists of Upper Pleistocene forced regressive wedge systems tracts (FRWST) deposits (Hunt & Tucker 1992).

Above unconformity ES, seismic profiles show relatively continuous, parallel and subparallel reflectors, gently inclined towards the SE as a result of low-angle backstepping and aggrading of layers. This unit is represented from bottom to top by the transgressive systems tract (TST) and highstand systems tract (HST) deposits that formed in response to the transgressive landward shift of the coastline during the rapid sea-level rise that accompanied the last deglaciation (c. 18–6 ka). The thickness of the uppermost Pleistocene–Holocene shelf wedge varies in the study area from 35–40 m in the inner–mid-shelf, to a minimum of 4–2 m at the shelf edge.

The HST deposits of the southern shelf of the Sorrento Peninsula between Amalfi and Capo d'Orso are characterized by the occurrence of a number of remarkably developed reflectors that can be correlated with different pyroclastic layers interbedded mostly within the upper Holocene succession. According to recent tephrostratigraphic (Buccheri *et al.* 2002; Insinga 2003; Sacchi *et al.*

2005; Insinga *et al.* 2008) and sequence stratigraphic research (Conforti 2003; Sacchi *et al.* 2004, 2005) conducted on the eastern Tyrrhenian margin off the Campania region these beds may be correlated to major tephra layers that originated from explosive eruptions of Somma–Vesuvius, the Campi Flegrei and Ischia. In particular, the seismic signature of the late HST deposits in the entire northern Bay of Salerno is characterized by a remarkable seismic horizon bounded by two high-amplitude reflectors that can be correlated with tephra layer tS2 deposited offshore during the AD 79 eruption of Vesuvius (Sacchi *et al.* 2005; Insinga *et al.* 2008) (Figs 12–26). The thickness of the tS2 tephra horizon ranges from a maximum of about 200 cm in the shoreface area off the Amalfi coast to some 10 cm at the shelf edge (Fig. 12).

Seismic profiles showed that the late HST (Upper Holocene) succession of the Amalfi shelf is characterized by a number of small prograding deltas that develop at the mouth of the small bedrock rivers with torrential regime. The best developed deltaic wedges in the study area occur at the mouth of the Regina Major torrent, offshore Maiori; at the mouth of the Regina Minor, off the

village of Minori; and at the mouth of Canneto, Dragone and Cappuccini torrents offshore Amalfi and Atrani. These deltaic bodies represent the subaqueous components of the confined alluvial fans that developed in the narrow coastal plain and pocket beaches of the Amalfi coast (see Fig. 4).

The Regina Major fan-delta

Offshore Maiori the thickness of the post-glacial succession is of the order of 50 ms. In particular, the HST deposits on the Maiori mid-shelf are significantly thicker than the correlative layers off the cliffed coast of Capo d'Orso and may exceed 35 ms (Fig. 14). The best throughgoing reflectors are represented by the *c.* 2 m thick seismic horizon bounded by reflectors F–H that is readily correlated with the pyroclastic fall of the AD 79 eruption of Vesuvius (tS2), and reflectors E (tephra tS1-γ), I (tephra tS3) and L (tephra tS3-α). Towards the inner shelf, a well-developed fan-delta is imaged by seismic profiles, which extends for *c.* 800 m from the mouth of the Regina Major torrent (Figs 15–19). The delta is characterized by sigmoid prograding foresets and a bottomset
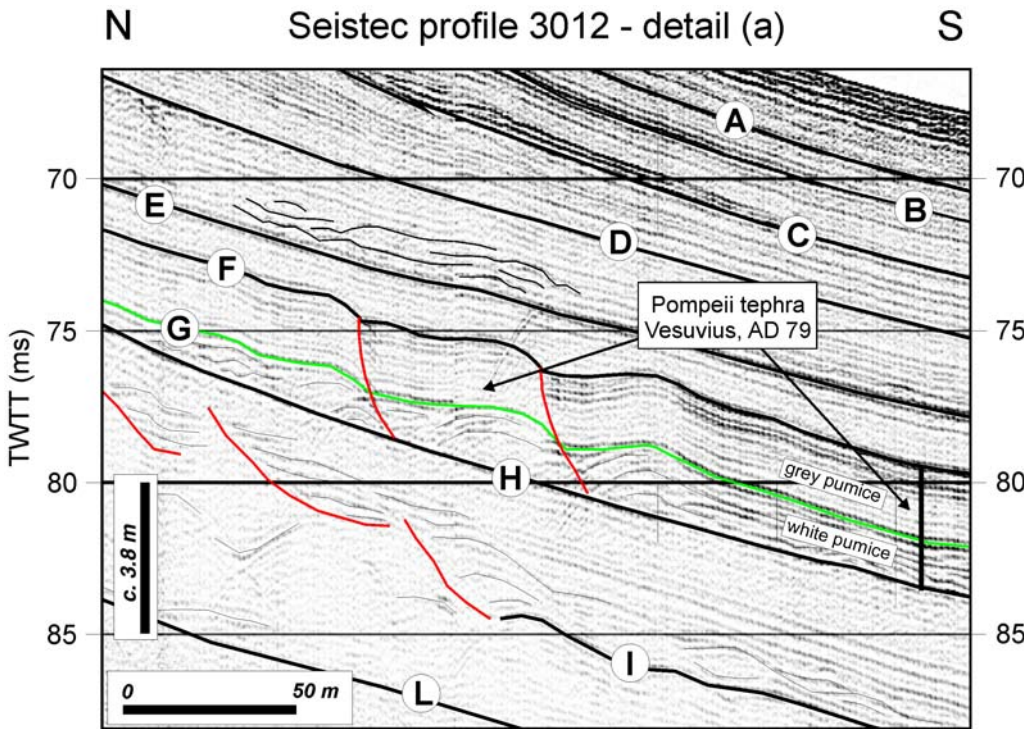
Fig. 15. Detail of Seistec profile 3012 showing the failure of the tephra bed deposited by Vesuvius 25 August, AD 79 ('Pompeii' eruption). (Note the fault-slumping of the tephra layer in the evacuation zone.) Figure 14 shows location and key to reflector labels.
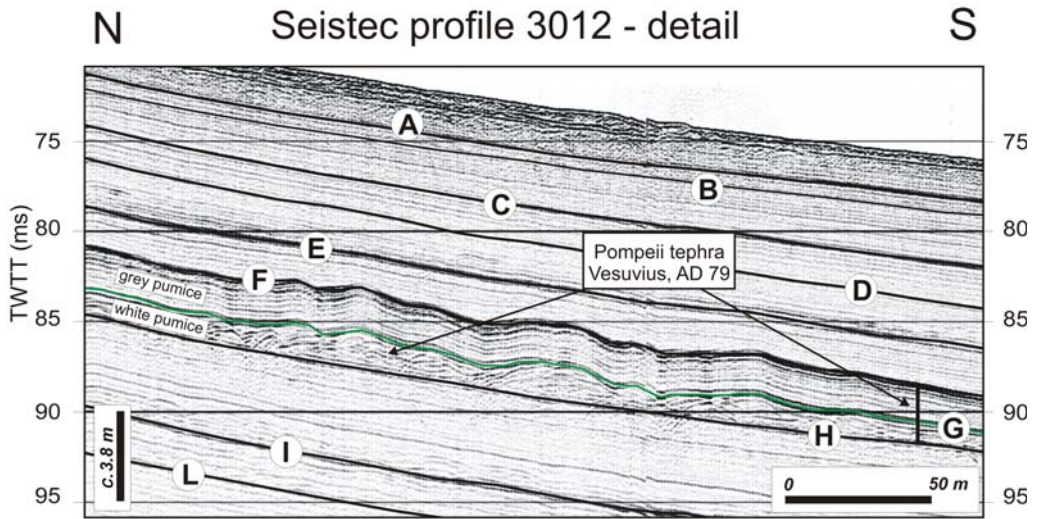
Fig. 16. Detail of Seistec profile 3012 showing the slumping of the Pompeii tephra bed (AD 79). (Note the soft-sediment deformation within the lower part of the tephra layer (i.e. white pumice), associated with detachment and sliding of the bed above its basal surface soon after its deposition.) Figure 14 shows location and key to reflector labels.
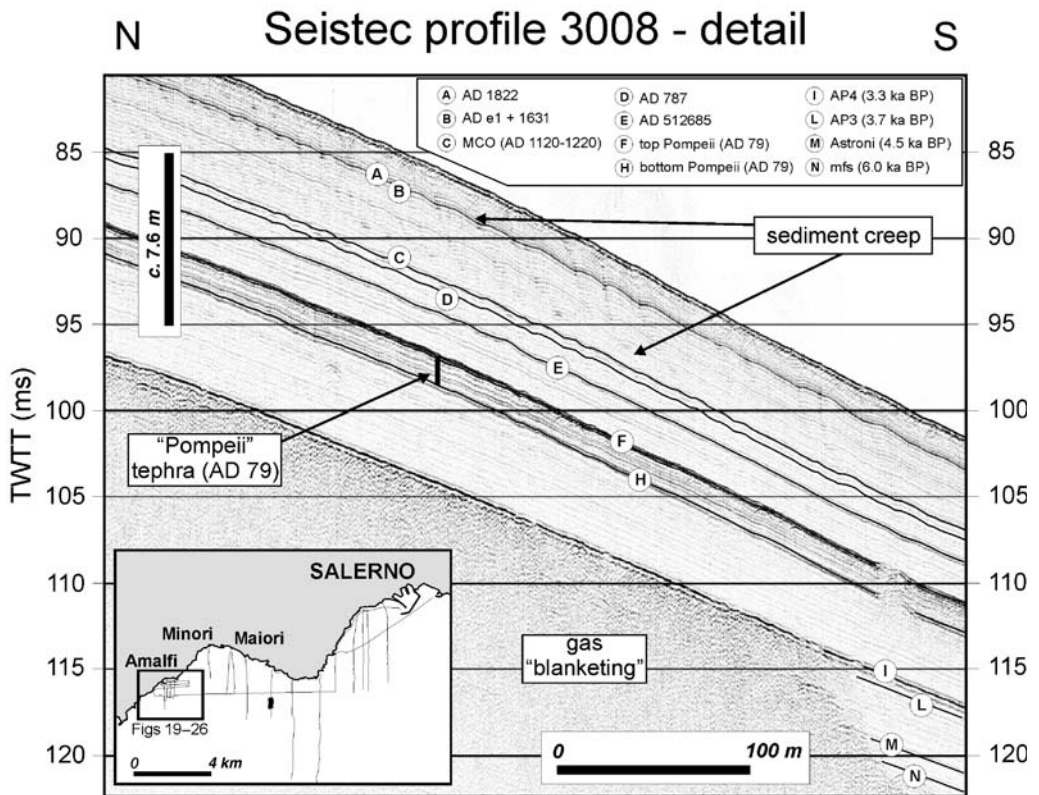
Fig. 17. Detail of Seistec profile 3008 showing crenulation of reflectors as a result of creep within the upper HST deposits of the prodelta area, mostly above the AD 79 ('Pompeii') tephra bed. Inset shows location of profile.
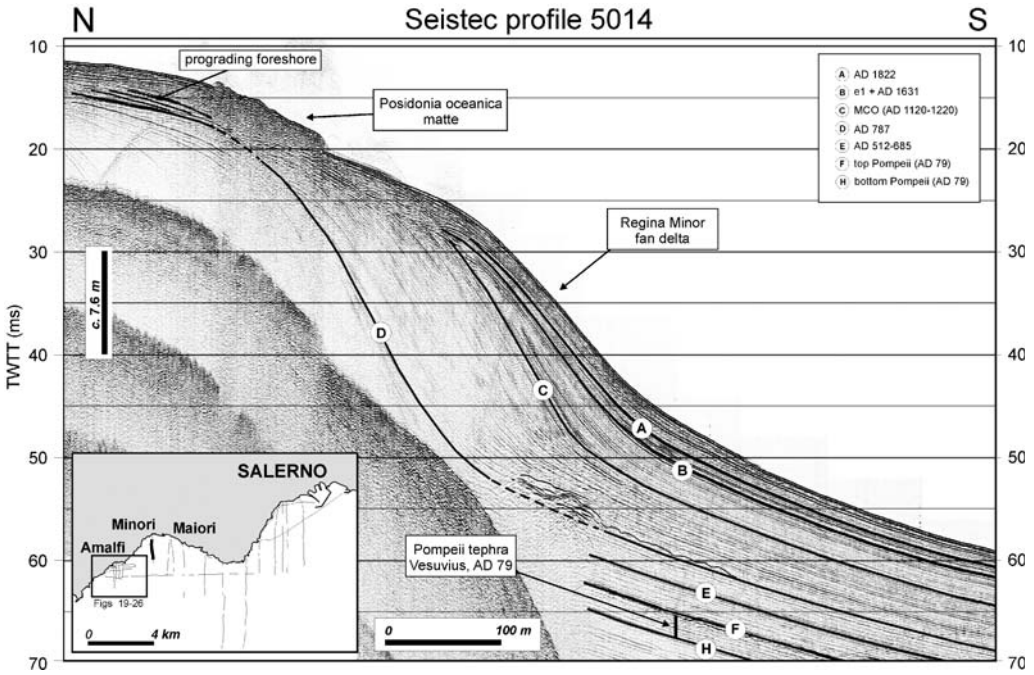
Fig. 18. Seistec profile 5014 off the Regina Minor stream mouth and its interpretation. (Note gravity-flow deposits above reflector D.) Inset shows location of profile.
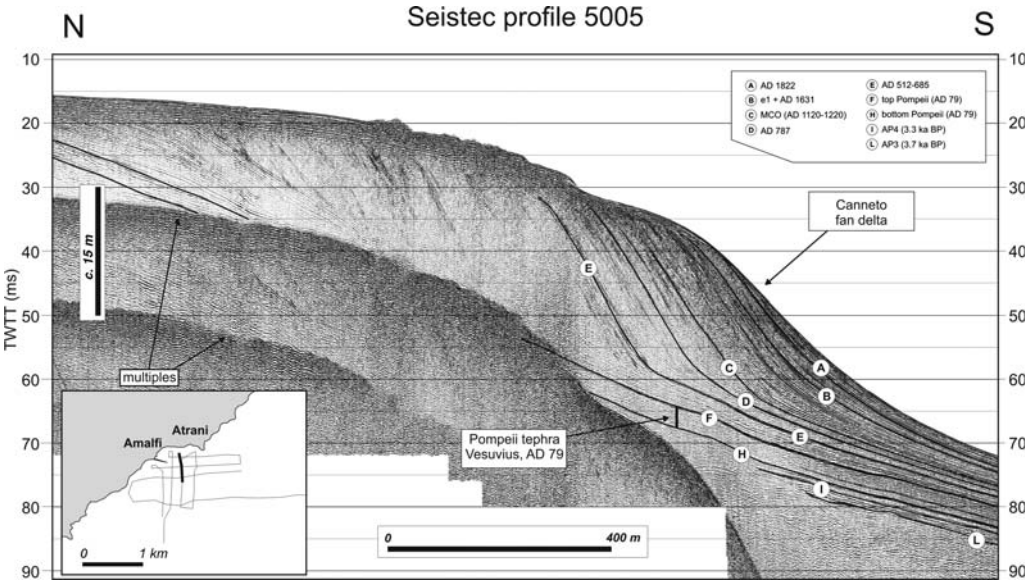
Fig. 19. Seistec profile 5005 offshore the Canneto stream, Amalfi, and its interpretation. Reflector E separates two different phases of development of the Canneto fan-delta. Inset shows location of profile.
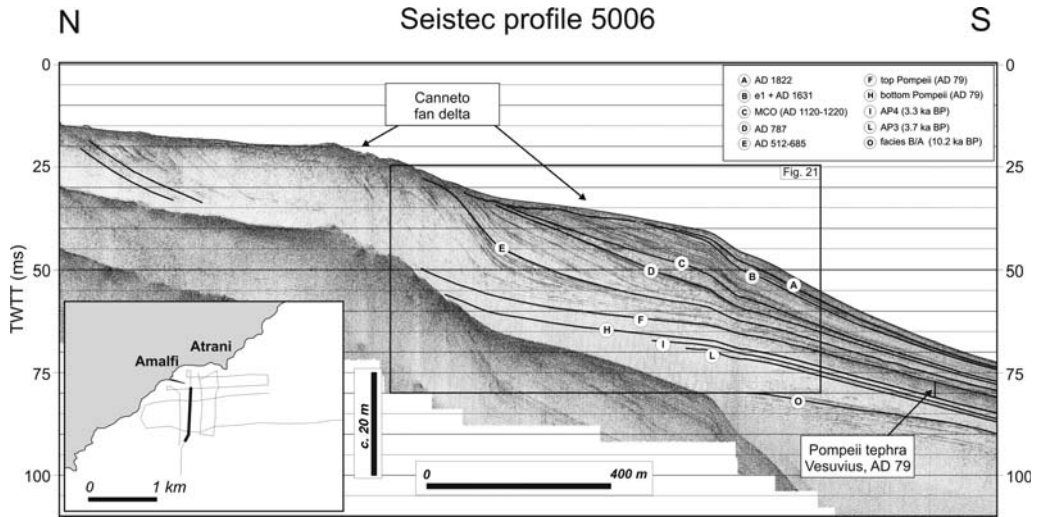
Fig. 20. Seistec profile 5006 offshore the Canneto stream, Amalfi, and its interpretation. (Note the significant growth of the fan-delta between reflectors F and E, together with the difference in the stratal architecture between the two parts of the deltaic body separated by horizon E.) Inset shows location of profile.

represented by the top of the AD 79 tephra layer. Inclination of foresets is between 10° in the inner fan-delta and 30° towards the delta front, whereas the present-day delta front slope is *c.* 20°.

Seistec profile 3012 documents the occurrence of sedimentary structures at the base of the Regina Major delta front that may be associated with a general gravity-driven instability and soft-sediment deformation above distinct stratigraphic surfaces, represented by reflector H (base of AD 79 pumice layer) and reflector I. Minor, but still clear evidence of sea-floor instability can be recognized above reflectors L and E (Fig. 14). Seismic interpretation suggests that soft-sediment deformation above the base of tephra tS2 mostly involves the pyroclastic layer itself and consists of slump–slide folding
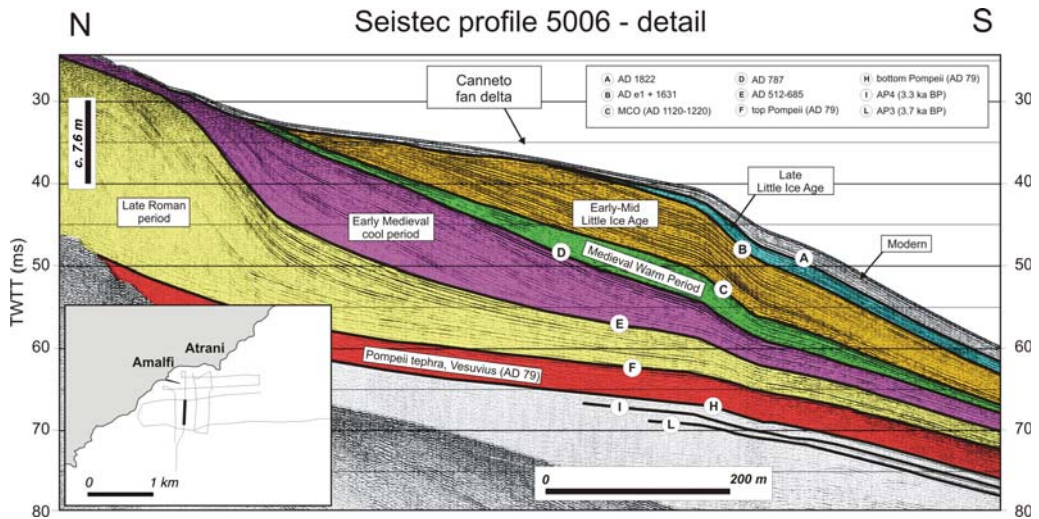
Fig. 21. Detail of Seistec profile 5006 off the Canneto stream, Amalfi, showing approximate correlation of prograding delta units with major climatic changes of the last 2000 years. (Note the backstepping and aggradation of strata within the stratigraphic unit corresponding to the apex of the Medieval Warm Period, which represents an exception to the generally prograding units of the fan delta.) Inset and Figure 20 show location.
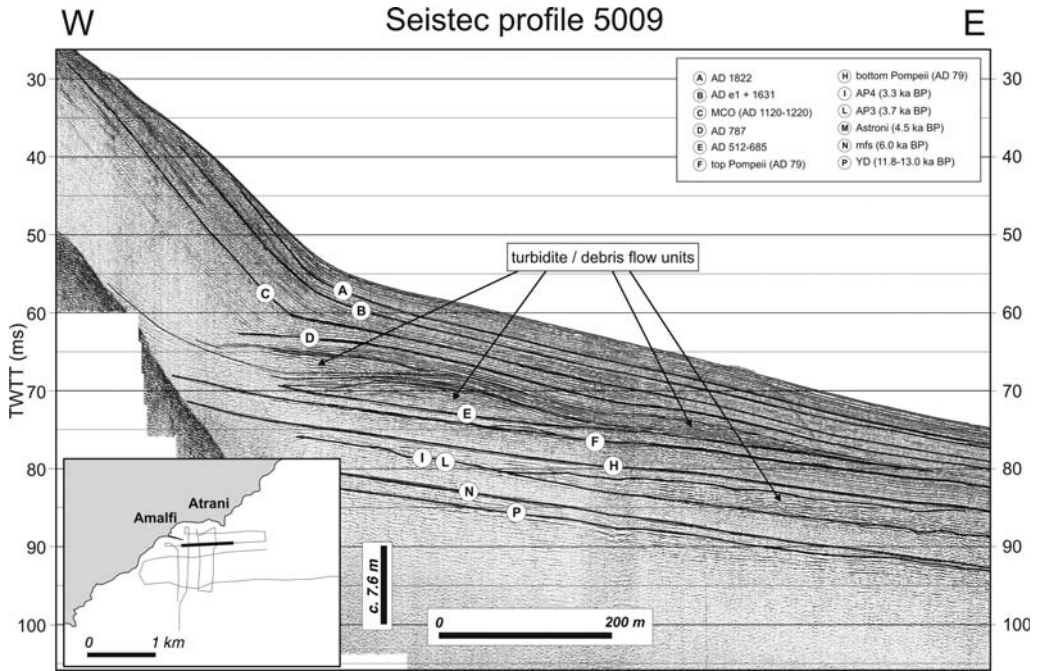
Fig. 22. Seistec profile 5009 offshore the Canneto stream, Amalfi, showing turbidite lobes or debris flow units occurring above different tephra layers (reflectors I, F and E). Inset shows location of profile.
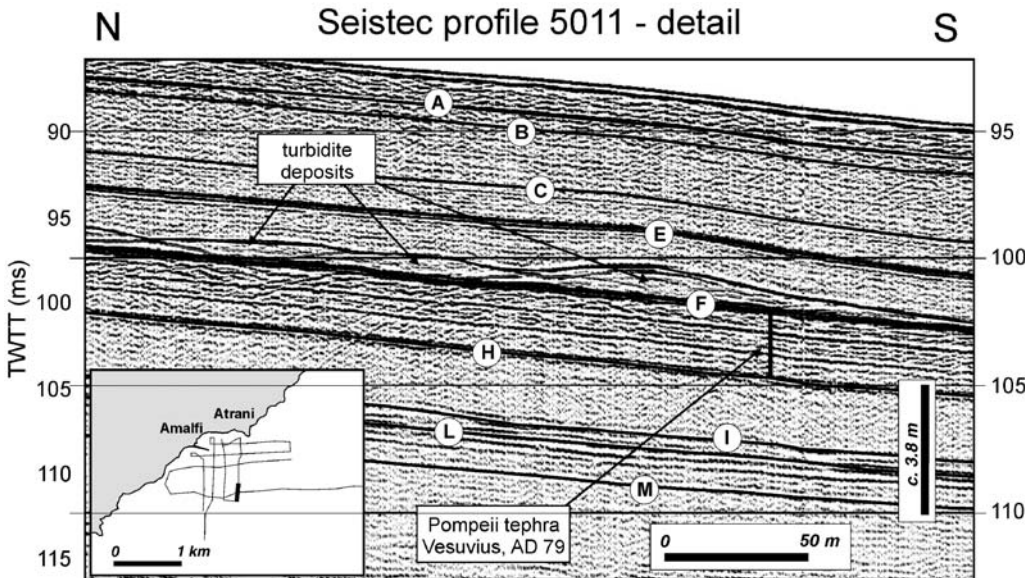
Fig. 23. Detail of Seistec profile 5011 off the Canneto fan prodelta showing distal fine-grained turbidites above the Pompeii (AD 79) tephra bed. Inset shows location of profile, and Tables 2 and 3 give legend for event beds.
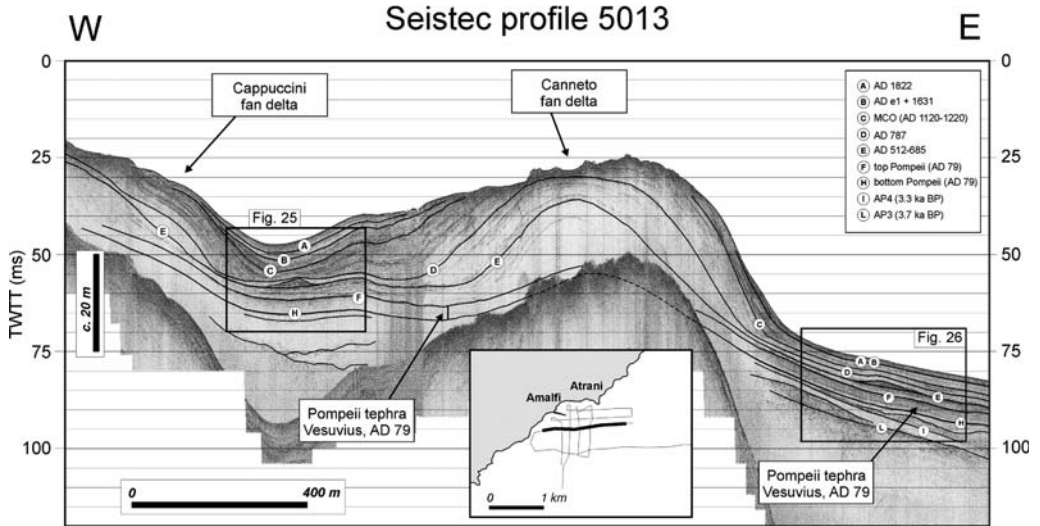
Fig. 24. Seistec profile 5013 offshore Amalfi showing a transverse section of the Cappuccini–Canneto delta system. (Note the development of turbidite and debris-flow units above different tephra layers (reflectors E, I and L).) Inset shows location of profile.

and slump–fault rupture of the tephra layer (Figs 14–16). The AD 79 pyroclastic unit is sandwiched between normal flat-lying dipping layers. The wavelength of the slump-folds is 20–60 m,

and fold amplitude is of the order of 0.5–1.0 m (Figs 15 and 16).

At a lower stratigraphic level other evidence exists of sediment failure, represented by hummocky
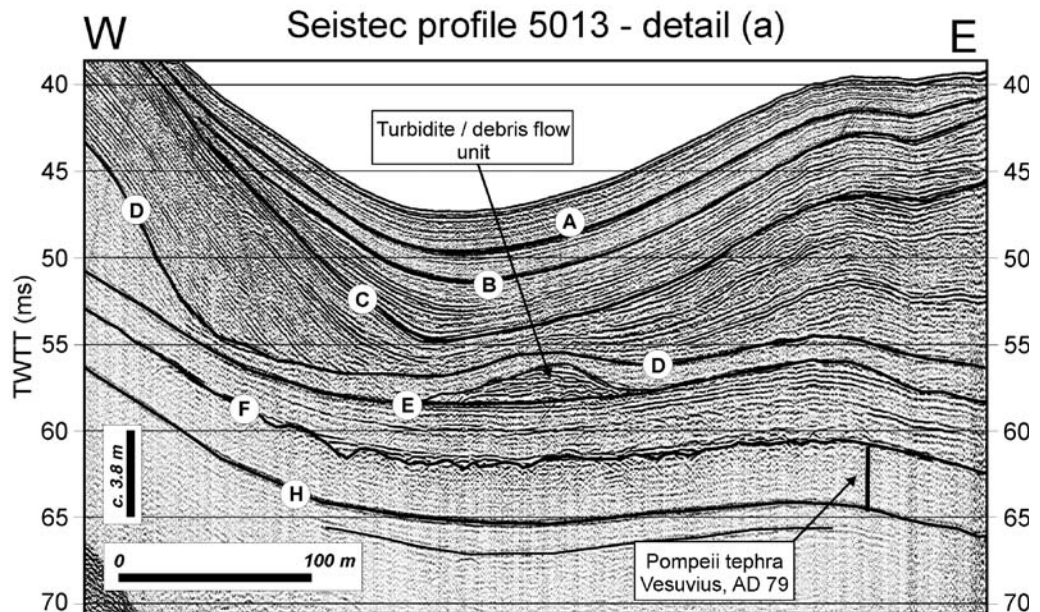
Fig. 25. Detail of Seistec profile 5013 showing turbidite and debris-flow deposits above seismic horizon E (tephra layer tS-1γ) in the channel between the Cappuccini and Canneto fan-deltas. Figure 24 shows location and key to reflector labels.
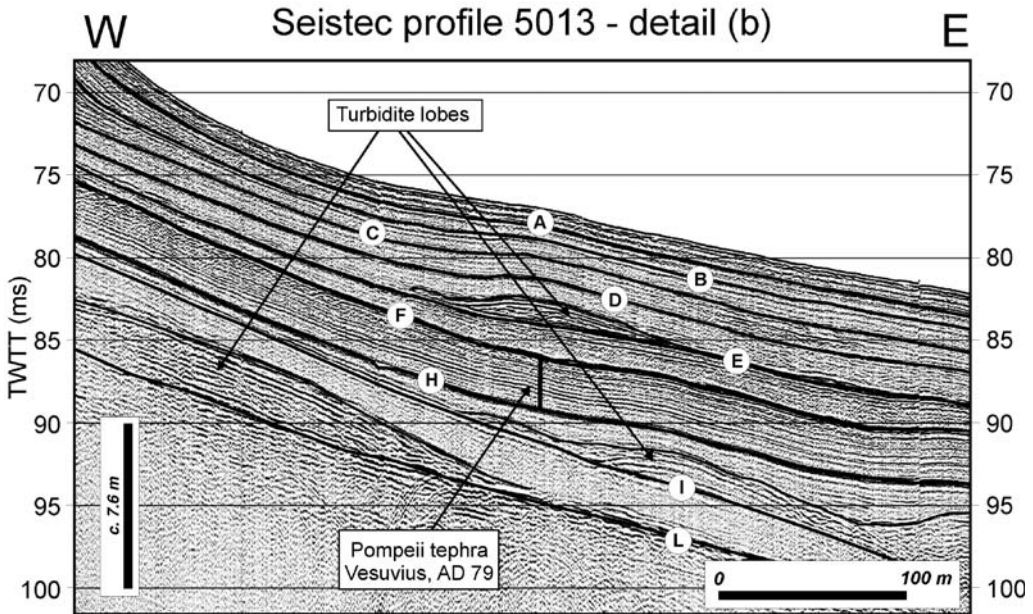
Fig. 26. Detail of Seistec profile 5013 off the Canneto fan-delta showing turbidite units deposited above different tephra layers (seismic horizons E, I and L). Figure 24 shows location and key to reflector labels.

bedforms with internal chaotic seismic facies that can be interpreted as slide or debris-flow deposits accumulated at the base of the delta front (Fig. 14). The sediment slide accumulation is sandwiched between seismic horizons H and I. Single hummocks are 50–100 m wide and up to 3 m high. Further evidence of sediment failure is also found above reflector N (maximum flooding surface), before the onset of the Holocene fan-delta *sensu stricto* (Fig. 15). Seismic profiles also indicate the occurrence of irregular geometry and crenulation of reflectors within the upper HST deposits of the prodelta area, mostly above reflector F (Fig. 17).

The Regina Minor fan-delta (Minori)

Adjacent to Maiori, off the village of Minori there is a major embayment of the Amalfi coast that hosts the westernmost part of the relatively large continental shelf of the northern Bay of Salerno, with a shelf break located at *c.* 3.5 km from the coast. Seistec profile 5014 shows a *c.* 50 ms (*c.* 40 m) thick post-glacial succession over the mid-shelf, and a well-developed fan-delta towards the inner shelf, as the underwater counterpart of the confined alluvial fan fed by the Regina Minor stream (Fig. 18).

The Regina Minor fan-delta is *c.* 800 m wide and the base of the foresets is about 500 m from the

Minori seashore. The pattern of seismic reflectors indicates that the stratigraphic architecture of the deltaic wedge is characterized, mostly above reflector F, by an average increase coupled with significant variations of progradation rates in the delta foresets. These variations are particularly evident in the delta front area (Fig. 18).

A pronounced step in the sea-bed morphology associated with chaotic internal reflections in the fan-delta topset area between 15 and 20 ms (*c.* 11–15 m water depth) is visible from seismic profile 5014 and can be interpreted as the result of the occurrence of a *Posidonia oceanica* 'meadow' that colonizes the sea floor (Fig. 18). It may also be observed from the seismic record that the meadow exerts a 'damming effect' and protects the modern foreshore from erosion by storm waves, thus allowing for the development of the foreshore sediment fill landward of the *Posidonia* meadow. The small prograding unit downlapping above reflector D landward of the *Posidonia* meadow may be thus interpreted as the product of a temporary seaward migration of the outer foreshore deposits during a period of coastline progradation.

Minor evidence of gravity-driven deformation is found at several stratigraphic levels towards the base of the delta front, above reflector D, and small-scale, creep-like, slope instability may be recognized at the top of the AD 79 tephra layer (reflector F) (Fig. 18).

The Canneto–Dragone fan-delta system (Amalfi–Atrani)

Off Amalfi and Atrani the width of the continental shelf is reduced to less than 2 km. The post-glacial succession offshore Amalfi–Atrani reaches a maximum thickness of *c.* 25 ms (*c.* 20 m) and is significantly thinner than in the adjacent sector off Minori and Maiori. Seismic correlation between the two sectors was ensured by a cross-check of the dip seismic profiles with the tie section 5004, which allowed tracing of the main Holocene reflectors across the entire Amalfi shelf. In this area seismic interpretation shows the occurrence of a sedimentary apron formed by the coalescence of two fan-deltas developing at the mouth of Torrente Canneto (Amalfi) and Torrente Dragone (Atrani), and a smaller delta representing the offshore extension of a small alluvial fan at the mouth of the Cappuccini torrent, immediately west of Amalfi harbour. The fan-delta system extends for about 1.5 km, from the mouth of the Dragone to that of the Cappuccini torrent, with delta-front foresets developing as far as 700 m from the coastline (Figs 19–26).

As in the cases of the Regina Major and Regina Minor fan-deltas, the AD 79 tephra horizon (tS2) marks a significant increase in the average prograding rates of foresets, which may be associated with a coarsening of the sediments entering the fan-delta system. Dip sections across the delta system show that the Canneto–Dragone prograding wedge may be divided into two sub-units by a downlap surface represented by reflector E. The two sub-units of the prograding wedge probably represent different phases in the development of the fan-delta system (Figs 20, 21 and 24–26).

Evidence of gravity-driven instability is common at various stratigraphic levels in the front of the Canneto–Dragone–Cappuccini delta system, particularly at the base of the prograding foresets, above horizons E, F and I–L. Seistec profiles show that gravity flows above horizon E locally form debris-flow units and/or turbidite lobes with a thickness of a few metres and width of a few tens of metres (Figs 22 and 24–26). Fine-grained turbidites are found above the AD 79 tephra layer, as suggested by the internal seismic facies and the external geometry of the deposits (Fig. 23).

Profile 5013 displays the stratigraphic architecture of the Canneto–Dragone–Cappuccini fan-delta system along strike and illustrates the occurrence of gravity-flow deposits above reflector E (Figs 24–26).

Discussion

Fan-deltas that develop along tectonically elevated, cliffed coasts at the mouth of ephemeral streams of temperate regions are typically fed by small alluvial fans, which are often confined in narrow, deeply incised V-shaped coastal valleys (Dabrio 1990; Nava-Sanchez *et al.* 1999; Fernández-Salas *et al.* 2003; Lobo *et al.* 2006). In these morphological settings the development and progradation of such small deltas generally have little or no subaerial expression. Furthermore, the recognition of their underwater component has often been hampered by the intrinsic resolution limits of the standard sub-bottom profiling, where coarse-grained deposits, shallow water and often gas saturation prevail. This is probably the reason why, until recently, these deltas have been mostly neglected by researchers in the outcrop and rarely described in the Holocene marine record (e.g. Prior & Bornhold 1990). Consequently, fan-deltas similar to those described in this study may be much more common than previously believed along cliffed coasts or even in deep inland lakes.

The IKB-Seistec seismic reflection profiles and gravity-core data used in this study have revealed unprecedented detailed views of the inner–mid-shelf depositional system of the northern Bay of Salerno, allowing the recognition of a number of fan-deltas that developed mostly during the last 2000 years, at the mouth of small rivers of the Amalfi cliffed coast. The deltaic bodies described in this study are small-scale fan-deltas, of about 1 km^2 area and a few tens of metres thick. They display a general conical morphology with a delta-front slope of *c.* 20° and foreset inclination between 15° and 30°. These bodies represent the underwater counterparts of coastal alluvial fans fed by small bedrock rivers with torrential regime that are part of the hydrographic network of the Sorrento Peninsula. These coastal alluvial fans are grouped at the seaward termination of the coastal gorges that dissect the tectonically elevated mountain range of the Lattari Mts., where virtually all land-derived sediment is deposited below sea level. In this context subaerial delta-plain components are practically absent and the narrow space at the exit of the valleys is filled with a coarse-grained alluvial prism up to a few tens of metres thick, whereas at the seashore the alluvial deposits are reworked into pocket-beach settings. Most of the modern settlements of the coastal villages of Maiori, Minori, Atrani and Amalfi are built on such deposits.

There is evidence in the literature suggesting that the dynamic regime of the alluvial fans of the Sorrento Peninsula–Amalfi coast is controlled by episodic, but often catastrophic sediment and water discharges that have caused repeated flooding of the fans in recent millennia (Esposito *et al.* 2004*a, b,* and references therein; Porfido *et al.* 2009; Violante *et al.* 2009). The ephemeral streams

that feed the alluvial fan systems are subject to episodic sheet wash and flash floods that may cause accumulation of large volumes of sediment. This is caused by heavy rains generated by the seasonal change of the atmospheric circulation in the Mediterranean region. The episodes of catastrophic rain typically bring very large sediment volumes to the fan-delta and offshore. This was the case for the catastrophic floods that struck the Amalfi coast between 25 and 26 October 1954, causing over 300 deaths (Esposito *et al.* 2004*a*). Following this dramatic event the coastline at the mouth of Bonea Stream, in Vietri, prograded seaward for more than 100 m (Esposito *et al.* 2004*a*, *b*, and references therein; Violante *et al.* 2009).

Seismic interpretation suggests that the general stratigraphic architecture of the studied fan-deltas is of two types. The deltaic bodies off Maiori and Minori display relatively steep and long sigmoidal foresets, commonly associated with topset layers. The fan-deltas off the Amalfi−Atrani coast show a clear variation in the dip angle of foresets and a very reduced or absent topset towards the delta fronts.

Another interesting observation on the overall stratal architecture of the fan-deltas is the remarkable regularity and lateral continuity of layers within the prograding foresets, so that the general 3D image of the deltaic bodies may be simply represented by a number of smooth, conical to hemispherical, onion-like layered underwater fans. Apparently, seismic profiles show no significant evidence of the various features or morphological zones typically associated with many coarse-grained marine deltas, such as distributary channels, gravel chutes or swales, flutes, stacked or switched sandy lobes, etc. In other words, seismic interpretation suggests that there is a lack of a system for delivering sediments towards deeper environments. Gravity-flow (inertia and/or turbidity flow) dominated transport of sediment proceeding directly from the coastal edge may be the primary cause for a substantial bypass of the sediment load to the lower slope segment, rather than segregation into distributary subsystems (Postma *et al.* 1988; Postma 1990, 1995; Parsons *et al.* 2001; McConnico & Bassett 2007).

The results of the seismic survey and the stratigraphic analysis on gravity-core samples suggest that the major changes in the stratal patterns within the fan-deltas of the Amalfi coast are often associated with the occurrence of single or clustered tephra layers interbedded within the Holocene record. In fact, all the fan-deltas described in this study started to develop above the pyroclastic bed deposited by Vesuvius during the 'Pompeii' Plinian eruption of AD 79. A significant change in the stratal architecture of the fan-deltas occurred after another eruption of Vesuvius, during the early Medieval period (*c.* AD 512−685). This is

documented by the development of a downlap surface that can be correlated with the oldest Medieval products of Vesuvius preserved in the Bay of Salerno (tephra layer tS1-γ). The seismic reflector (E) that correlates with these products consistently separates the fan-deltas of all the study areas into two sub-units showing distinct stratal patterns (see Figs 19−21). Furthermore, minor changes in the stratal patterns of the fan-delta system may be recognized within the upper (early Medieval) sub-unit, as illustrated in Figure 21.

Seistec profiles reveal evidence of gravity-driven instability at various stratigraphic levels within the fan-deltas. All the observed features are not randomly distributed in the stratigraphic record but appear concentrated along distinct stratigraphic horizons or intervals. Probably, more than one mechanism of sediment deformation or failure could explain the variety of the features described in the fan-deltas of the Amalfi coast and a thorough discussion of such mechanisms would require a better control on mechanical properties of the sediment involved (e.g. Sultan *et al.* 2004). The available data allow for the recognition of (1) crenulation in mud-dominated prodelta slopes, possibly associated with shear deformation of sediments by creeping; (2) slide or slump deformation of the AD 79 pyroclastic deposits; (3) gravity (inertia, turbidity or debris) flow deposits associated with selected stratigraphic intervals.

Crenulation in mud-dominated prodelta slopes

Irregular geometry and crenulation of reflectors within horizons or packages above reflector H, in the prodelta area, have been detected on seismic profiles off the Regina Major fan-delta. This is particularly clear in the upper HST deposits, above a basal surface represented by the Pompeii tephra of AD 79 (Fig. 17).

According to several reports, sea-floor crenulations are common in mud-dominated prodelta slopes offshore river mouths all around the Mediterranean and elsewhere (Correggiari *et al.* 2001; Lee *et al.* 2002). In some cases the stratal geometry of such crenulations may resemble typical sand-wave morphology, and the origin of these features has been regarded as controversial. They may occur under sea-floor gradients of tenths of a degree, display a variety of internal geometries and seem to be associated with high sedimentation rates (Correggiari *et al.* 2001; Canals *et al.* 2004; Cattaneo *et al.* 2004; Trincardi *et al.* 2004).

In the case of the Regina Major prodelta the lack of conspicuous sandy facies in any of the cores collected through the basal surface does not provide evidence in favour of the hypothesis of a buried field of sandy bedforms. Hence it may be proposed

that the crenulations imaged by Seistec profiles represent the effect of gravity-driven deformation as a result of creep of the upper HST above a basal surface represented by the Vesuvius AD 79 tephra.

Slide or slump deformation of the AD 79 pyroclastic deposits

Offshore Maiori, seismic profiles have revealed significant gravity-driven deformation involving AD 79 tephra layer. In particular, stratal geometries highlight evidence for the slumping of the entire 2 m thick tephra layer by extensive shear deformation as a result of partial detachment from its base, along with internal deformation of the lower part of the tephra bed (white pumice), probably caused by the load exerted by the upper part (grey pumice) soon after its rapid deposition (Figs 14–16). The seismic records clearly image the slumped AD 79 pyroclastic unit sandwiched between normal flat-lying dipping layers. The longer wavelength of the slump-folds is 20–50 m, and fold amplitude is of the order of 1–2 m. Similar examples of slumping of volcaniclastic beds deposited underwater have been described, for instance, in the pyroclastic deposits that crop out at Lake Mono (Miller *et al.* 1982; Miller 1989).

It appears that the slump-fold deformation of the Pompeii tephra off the Regina Major stream was caused by the loading associated with the highly water-saturated, 2 m thick pyroclastic layer on the fan-delta slope. According to recent reconstructions, the pyroclastic bed was deposited within less than 12 h between the early afternoon and the night of 24 August, AD 79 (Dal Maso *et al.* 1999). Such extremely rapid, largely undrained loading over the underwater delta slope was probably responsible for a rapid decrease in the shear strength at the base of the layer and the consequent slump-fold deformation of the whole unit.

Gravity (inertia, turbidity or debris) flow deposits associated with selected stratigraphic intervals

Slope instability is also documented on seismic profiles by the repeated occurrence at different stratigraphic levels of sediment prisms probably corresponding to accumulation of gravity flow-type deposits. These deposits are typically found at the base of the delta front and may range in size from a few cubic metres to several hundreds of cubic metres. According to seismic interpretation they do not occur randomly but, again, are mostly concentrated along specific stratigraphic levels. From bottom to top, gravity-flow deposits tend to occur

above tephra layers; namely, tS4 (Astroni) tS3-α (AP3), tS3 (AP4), tS2 ('Pompeii' tephra bed) and tS1-γ (early Medieval eruption) (Figs 18 and 24–26). There does not seem to be evidence of significant evacuation zones of sediments that eventually collapsed (or were eroded) from the delta front and were redeposited downslope by gravity flows. This may reinforce the previous suggestion that the studied fan-deltas lack major sediment segregation zones in the delta front and are dominated by effective bypass of alluvial sediments directly from the foreshore area to the lower segments of the fan-delta slopes.

Clues to mechanisms controlling underwater sediment dispersal

Notwithstanding the recent progress in the study of modern subaqueous coarse-grained, steep-faced deltas the general understanding of the sediment transport mechanisms operating on steep subaqueous slopes of coarse-grained deltas is still relatively limited (Nemec 1990*b*, 1995; Postma 1990; Mulder & Syvitski 1995; Mulder *et al.* 2003; Mutti *et al.* 2003). This is probably due, on the one hand, to the virtual inaccessibility of the subaqueous delta slopes to direct sedimentological observation and, on the other, to the limited examples of surveyed subaqueous deltas documented in the literature.

It is generally accepted that medium–coarse sediments may be transported for long distances away from nearshore fan-deltas. Side-scan sonar data have shown, for example, that during exceptional river floods the riverborne load appears to have sufficient energy to overcome buoyancy and frictional effects at the river mouth (Prior & Bornhold 1990). The near-bed concentrations of sediments appears to be largely unaffected by seawater density and may proceed across the subaqueous slopes as hyperpycnal flows. Where the bottom gradient of the nearshore fan is greater than the slope of the river thalweg, the offshore transport of gravel and sand is enhanced. In the foreshore area river-driven transport is in some places replaced by gravity-driven transfer of sediment along the underwater slopes. Hence coarse-grained sediment transport downslope over the fan may be significantly controlled by high-density, pseudolaminar inertia flows, and/or turbidity flows, as described experimentally by Postma *et al.* (1988) and proposed on the basis of modelling (Mulder & Syvitski 1995; Mulder *et al.* 2003) and outcrop studies on ancient deltas (Mutti *et al.* 2003; Plink-Bjorklund & Steel 2004).

Gravity flows usually originate in one of two ways: as surge-type sediment gravity flows generated by localized slope failure (Prior *et al.* 1987; Bornhold & Prior 1990; Nemec 1990*b*) or by more

sustained currents related to sediment-laden hyper-pycnal effluent (Gilbert 1975; Bornhold & Prior 1990; Chikita 1990; Mutti *et al.* 2003). In the case of the fan-deltas of the Amalfi coast, the absence of slide scars and evacuation zones landward of the flow deposits suggests that the principal mechanism for dispersal on the steep delta slopes is by sediment gravity flows, or highly concentrated mixtures of sediment and water moving close to the bed that probably evolve into turbulent flows during down-slope motion. These may include the whole spectrum of gravity-driven processes from debris flows to grain flows and even high-density turbidity currents as they build momentum down the foreset slope.

Effects of landscape-mantling volcaniclastic deposits on the river basin erosional dynamics

Seismic stratigraphic interpretation showed that most of the gravity-driven instability processes are not diffused across the fan-delta but are concentrated on a few stratigraphic horizons that invariably correspond to major tephra layers or tephra clusters. This observation, coupled with the recognition that the sediment supply to the fan-delta system is largely affected by high-energy river floods, suggests a direct relationship between the rates of erosion of the river basin slopes that follow deposition of landscape-mantling volcaniclastic deposits and the rates of underwater sediment that are delivered to the fan-deltas.

In fact, during and following subaerial eruptions, sediment erosion and delivery rates are typically high, not only because of the large volumes of unconsolidated material, but also because sediment-stabilizing vegetation is often destroyed or damaged. Landscape-mantling deposits, mostly airfall tephra, are deposited in comparatively thin sheets of unwelded pyroclastic deposits that mantle topography and/or cap sequences. These deposits are quickly eroded by sheetwash or rill and gully erosion and the sediment yield from these sources declines rapidly, within a few years, as the gullies reach permeable, less erodible substrates and resistant surface crust develops (Collins & Dunne 1986; Cinque & Robustelli 2009). However, it may be expected that the effects of accelerated slope erosion may last for several decades, or even longer. Valley-fill deposits, such as debris avalanche and volcaniclastic deposits, typically erode not from the surface but also from the side, thus causing channel widening or bank erosion and collapse. As a consequence, the newly formed rock debris may further enhance slope erosion rates and keep providing high sediment yields to the seashore for a relatively long time.

## Role of climatic forcing on the development of fan-deltas

It is widely documented that climatic changes significantly affect the stratal patterns of inner-shelf systems in general, and particularly deltaic settings, worldwide. In recent millennia, periods of cooler climate in the Mediterranean region were typically accompanied by periods of higher rainfall that may have resulted, in turn, in enhancing erosion on slopes. For instance, abrupt shifts between arid and humid phases are known to create temporary disequilibrium between climate, biotic processes and geomorphological processes, when rainfall erosivity is high and protective vegetation cover not fully established (e.g. Dabrio 1990; Mulder & Syvitski 1995; Fernández-Salas *et al.* 2003; Lobo *et al.* 2006).

The interpretation proposed in this study implies that the growth rates of the fan-deltas of the Amalfi coast were primarily controlled by the average recurrence interval and magnitude of river flooding episodes that have provided high sediment yields to the delta system, concomitant with periods during which abundant, erosion-prone (volcani)clastic material was available on the slopes of the river basins. Accordingly, it may be proposed that the amount of sediments delivered to the coastline and hence the rates of development of the Amalfi fan-deltas in the last 2000 years were possibly dictated by the interplay of the availability of loose pyroclastic cover on the slopes of the alluvial basins and the varying erosional rates on the slopes caused by the climatic oscillations that have occurred during recent millennia (Fig. 27).

In particular, the major change detectable in the stratal geometries of the fan-deltas occurring in the early Medieval time (tephra tS1-γ) may be associated with the onset of a period of climatic cooling, known as Early Medieval Cool Period (*c.* AD 500–800), that developed immediately after the Roman Warm Period. Further minor changes in the stratal patterns of the delta foresets, which are consistently imaged by the seismic record in all the fan-deltas of the Amalfi coast, may be tentatively correlated with the Medieval Warm Period (*c.* AD 900–1100) and the Little Ice Age (*c.* AD 1400–1850) (Fig. 21).

Conclusion

The interpretation of the very high-resolution (IKB-Seistec) seismic survey, calibrated with gravity-core data, showed that the fan-delta system imaged off the Amalfi rocky coast developed after the AD 79 Plinian eruption of Vesuvius. During this time interval of *c.* 2000 years, both sea-level oscillation
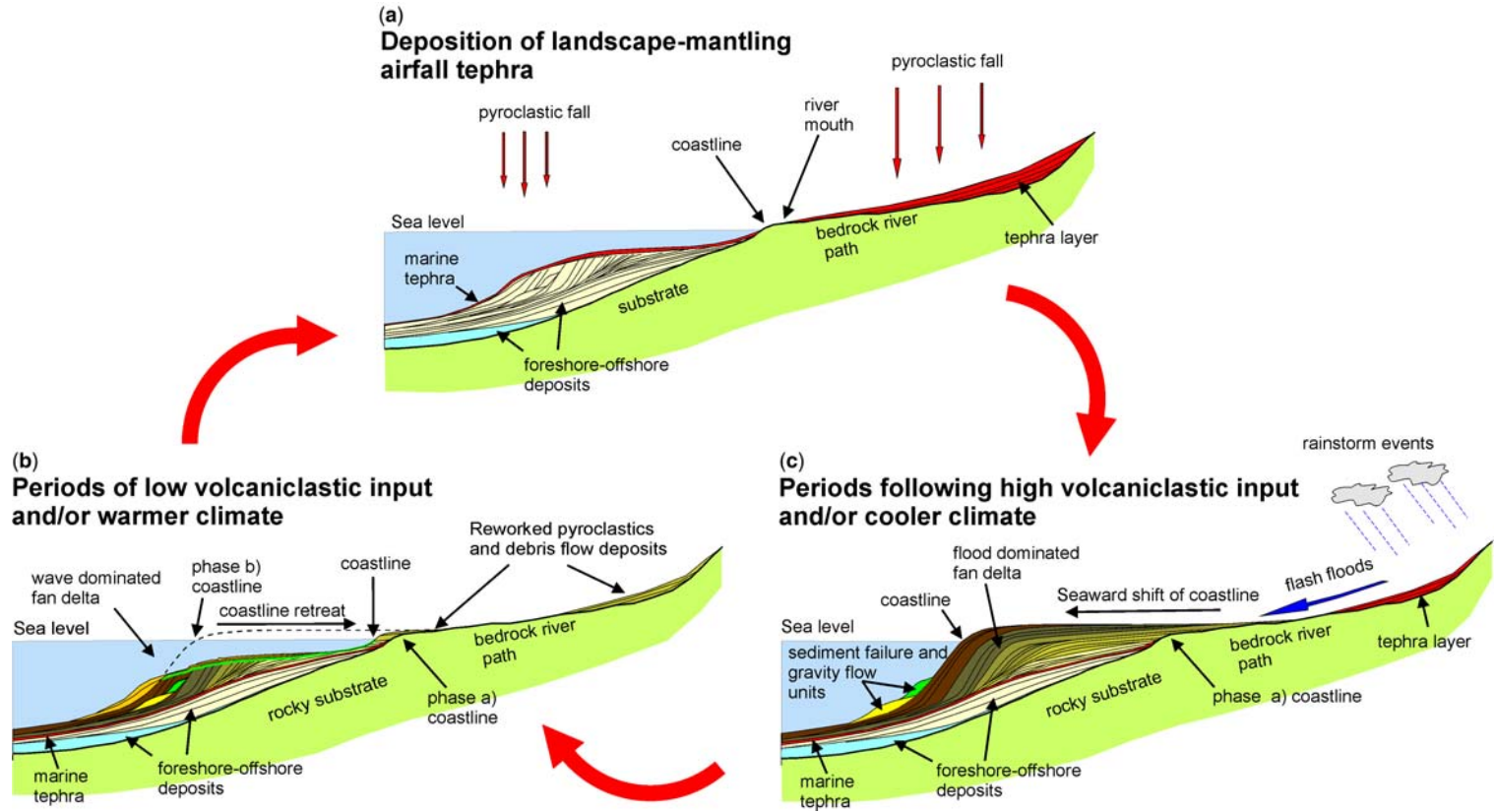
Fig. 27. Concept of Holocene delta growth cycles under varying climatic conditions and sediment input rates for mixed silicliclastic–volcaniclastic fan-deltas associated with Mediterranean-type cliffed coasts.

and tectonic subsidence or uplift were practically negligible in terms of influence on the overall stratigraphic architecture of the inner-shelf system, and the main factor controlling stratal geometries and patterns was the rate and mode of sediment supply.

The prominent gravity-driven instability and deformation of sediments detected at various stratigraphic levels within the delta slopes, along with the substantial lack of subaerial delta-plain components or other subaqueous segregation zones for sediments (e.g. distributary channels, levee complexes), suggest that the stratal geometry of the fan-deltas was dominantly dictated by the effective transfer of sediments by hyperpycnal (e.g. inertia, turbidity) flows directly fed by river flooding to the lower segments of the delta slopes.

The various phases of subaqueous delta growth were also controlled by the interplay of two main factors: (1) the accelerated erosion of slopes of the alluvial basins by sheetwash and flashfloods during and/or following periods of intense volcanism, which resulted in the delivery of considerable volumes of volcaniclastic debris and loose sediments to the shoreline; (2) the varying erosive potential of the river basin slopes under the changing morphoclimatic regimes over the last 2000 years.

References

ACOCELLA, V. & FUNICIELLO, R. 2006. Transverse systems along the extensional Tyrrhenian margin of central Italy and their influence on volcanism. *Tectonics*, **25**, TC2003, doi:10.1029/2005TC001845.

ANDRONICO, D. & CIONI, R. 2002. Contrasting styles on Mount Vesuvius activity in the period between the Avellino and Pompeii Plinian eruptions, and some implications for assessment of future hazards. *Bulletin of Volcanology*, **64**, 372–391.

ANDRONICO, D., CALDERONI, G., CIONI, R., SBRANA, A., SULPIZIO, R. & SANTACROCE, R. 1995. Geological map of Somma–Vesuvius volcano. *Periodico di Mineralogia*, **64**, 77–78.

ARRIGHI, S., PRINCIPE, C. & ROSI, M. 2001. Violent strombolian and sub-Plinian eruptions at Vesuvius during post-1631 activity. *Bulletin of Volcanology*, **63**, 126–150.

ASIOLI, A. 1996. High resolution foraminifera biostratigraphy in the Central Adriatic basin during the last deglaciation: a contribution to the PALICLAS Project. *In*: OLDFIELD, F. & GUILIZZONI, P. (eds) *Palaeoenvironmental Analysis of Italian Crater Lake and Adriatic Sediments*. Memorie dell'Istituto Italiano di Idrobiologia, **55**, 197–218.

ASIOLI, A., TRINCARDI, F., LOWE, J. J., ARIZTEGUI, D., LANGONE, L. & OLDFIELD, F. 2001. Sub-millennial scale climatic oscillations in the central Adriatic during the Lateglacial: paleoceanographic implications. *Quaternary Science Reviews*, **20**, 1201–1221.

BARTOLE, R., SAVELLI, D., TRAMONTANA, M. & WEZEL, F. C. 1984. Structural and sedimentary features in the Tyrrhenian margin off Campania, Southern Italy. *Marine Geology*, **55**, 163–180.

BISSON, M., PARESCHI, M. T., ZANCHETTA, G., SULPIZIO, R. & SANTACROCE, R. 2007. Volcaniclastic debris-flow occurrences in the Campania region (Southern Italy) and their relation to Holocene–Late Pleistocene pyroclastic fall deposits: implications for large-scale hazard mapping. *Bulletin of Volcanology*, **70**, 157–167.

BOLTOVSKOY, E. 1976. Distribution of Recent foraminifera in the South American region. *In*: HEDLEY, R. H. & ADAMS, C. G. (eds) *Foraminifera, 2*. Academic Press, London, 171–236.

BORNHOLD, B. D. & PRIOR, D. B. 1990. Morphology and sedimentary processes on the subaqueous Noeick River delta, British Columbia, Canada. *In*: COLELLA, A. & PRIOR, D. B. (eds) *Coarse-Grained Deltas*. International Association of Sedimentologists, Special Publications, **10**, 169–181.

BRANCACCIO, L., CINQUE, A., ROMANO, P., RUSSO, F., SANTANGELO, N. & SANTO, A. 1991. Geomorphology and neotectonic evolution of a sector of the Tyrrhenian flank of the southern Apennines (Region of Naples, Italy). *Zeitschsift für Geomorphologie*, **82**, 47–58.

BROWN, R. J., ORSI, G. & DE VITA, S. 2008. New insights into Late Pleistocene explosive volcanic activity and caldera formation on Ischia (southern Italy). *Bulletin of Volcanology*, **70**, 583–603.

BUCCHERI, G. 1984. Pteropods as climatic indicators in Quaternary sequences. A lower–middle Pleistocene sequence outcropping in Cava Puleo (Ficarazzi, Palermo, Italy). *Palaeogeography, Palaeoclimatology, Palaeoecology*, **45**, 75–86.

BUCCHERI, G., CAPRETTO, G. *ET AL.* 2002. A high resolution record of the last deglaciation in the southern Tyrrhenian Sea: environmental and climatic evolution. *Marine Geology*, **186**, 447–470.

BUDILLON, F., VIOLANTE, C., CONFORTI, A., ESPOSITO, E., INSINGA, D., IORIO, M. & PORFIDO, S. 2005. Event beds in the recent prodelta stratigraphic record of the small flood-prone Bonea Stream (Amalfi Coast, Southern Italy). *Marine Geology*, **222–223**, 419–441.

CANALS, M., LASTRAS, G. *ET AL.* 2004. Slope failure dynamics and impacts from seafloor and shallow

sub-seafloor geophysical data: case studies from the COSTA project. *Marine Geology*, **213**, 9–72.

CARALP, M. H. 1988. Size and morphology of the benthic foraminifera *Melonis barleeanum*: relationships with marine organic matter. *Journal of Foraminiferal Research*, **19**, 235–245.

CARBONE, A., LIRER, L. & MUNNO, R. 1984. Caratteri petrografici dei livelli piroclastici rinvenuti in alcuni gravity-cores nel Golfo di Pozzuoli e di Napoli. *Memorie della Società Geologica Italiana*, **27**, 195–204.

CAREY, S. & SIGURDSSON, H. 1987. Temporal variations in column height and magma discharge rate during the AD 79 eruption of Vesuvius. *Geological Society of America Bulletin*, **99**, 303–314.

CATTANEO, A., CORREGIARI, A., MARSSET, T., THOMAS, Y., MARSSET, B. & TRINCARDI, F. 2004. Seafloor undulation pattern on the Adriatic shelf and comparison to deep-water sediment waves. *Marine Geology*, **213**, 121–148.

CHIKITA, K. 1990. Sedimentation by river-induced turbidity currents: field measurements and interpretations. *Sedimentology*, **37**, 891–905.

CINQUE, A. & ROBUSTELLI, G. 2009. Alluvial and coastal hazards caused by long-range effect of Plinian eruptions: the case of the Lattari Mts. after the AD 79 eruption of Vesuvius. *In*: VIOLANTE, C. (ed.) *Geohazard in Rocky Coastal Areas*. Geological Society, London, Special Publications, **322**, 155–171.

CINQUE, A., AUGELLI, P. P. C. *ET AL.* 1997. Volcanism, tectonics and recent geomorphological change in the Bay of Napoli. *Geografia Fisica e Dinamica Quaternaria, Supplement*, **3**, 123–141.

CIONI, R., MARIANELLI, P. & SBRANA, A. 1992. Dynamics of the A.D. 79 eruption: stratigraphic, sedimentological and geochemical data on the successions from the Somma–Vesuvius southern and eastern sectors. *Acta Vulcanologica*, **2**, 109–123.

CIONI, R., SANTACROCE, R. & SBRANA, A. 1999. Pyroclastic deposits as a guide for reconstructing the multi-stage evolution of the Somma–Vesuvius caldera. *Bulletin of Volcanology*, **61**, 207–222.

CIONI, R., BERTAGNINI, A., SANTACROCE, R. & ANDRONICO, D. 2008. Explosive activity and eruption scenarios at Somma–Vesuvius (Italy): Towards a new classification scheme. *Journal of Volcanology and Geothermal Research*, **177**, 277–287.

COLELLA, A. & PRIOR, B. D. (eds) 1990. *Coarse-Grained Deltas*. International Association of Sedimentologists, Special Publications, **10**.

COLEMAN, J. M. 1988. Dynamic changes and processes in the Mississippi River Delta. *Geological Society of America Bulletin*, **100**, 999–1015.

COLEMAN, J. M. & PRIOR, D. B. 1982. Deltaic environments of deposition. *In*: SCHOLLE, P. A. & SPEARING, D. (eds) *Sandstone Depositional Environments*. American Association of Petroleum Geologists, Memoirs, **31**, 139–178.

COLLINS, B. D. & DUNNE, T. 1986. Erosion of tephra from the 1980 eruption of Mount St. Helens. *Geological Society of America Bulletin*, **97**, 896–905.

CONFORTI, A. 2003. *Stratigrafia integrata della sequenza Tardo-Quaternaria del settore settentrionale del Golfo di Salerno e di quello meridionale del Golfo di Napoli*. PhD thesis, University of Naples Federico II.

CORREGGIARI, A., TRINCARDI, F., LANGONE, L. & ROVERI, M. 2001. Styles of failure in late Holocene highstand prodelta wedges on the Adriatic shelf. *Journal of Sedimentary Research*, **71**, 218–236.

DABRIO, C. J. 1990. Fan-delta facies associations in late Neogene and Quaternary basins of southern Spain. *In*: COLELLA, A. & PRIOR, D. B. (eds) *Coarse-Grained Deltas*. International Association of Sedimentologists, Special Publications, **10**, 91–111.

DAL MASO, C., MATURANO, A. & VARONE, A. 1999. Pompei, il racconto dell'eruzione. *Le Scienze*, **371**, 58–65.

DI VITO, M., ISAIA, R. *ET AL.* 1999. Volcanism and deformation since 12,000 years at the Campi Flegrei caldera (Italy). *Journal of Volcanology and Geothermal Research*, **91**, 221–246.

DI VITO, M. A., SULPIZIO, R., ZANCHETTA, G. & D'ORAZIO, M. 2008. The late Pleistocene pyroclastic deposits of the Campanian Plain: new insights into the explosive activity of Neapolitan volcanoes. *Journal of Volcanology and Geothermal Research*, **177**, 19–48.

DROSER, M. J. & BOTTJER, D. J. 1991. Trace fossils and ichnofabric in Leg 119 cores. *In*: BARRON, J., LARSEN, B. *ET AL.* (eds) *Proceedings of the Ocean Drilling Program, Scientific Results, 119*. Ocean Drilling Program, College Station, TX, 635–641.

EINSELE, G. 2000. *Sedimentary Basins: Evolution, Facies and Sedimentary Budget*. Springer, Berlin.

ESPOSITO, E., PORFIDO, S. & VIOLANTE, C. (eds) 2004*a*. *Il nubifragio dell'ottobre 1954 a Vietri sul Mare, Costa di Amalfi, Salerno*. Pubblicazione Gruppo Nazionale per la Difesa dalle Catastrofi Idrogeologiche, **2870**.

ESPOSITO, E., PORFIDO, S., VIOLANTE, C., BISCARINI, C., ALAIA, F. & ESPOSITO, G. 2004*b*. Water events and historical flood recurrences in the Vietri sul Mare coastal area (Costiera Amalfitana, southern Italy). *In*: RODDA, G. & UBERTINI, L. (eds) *The Basis of Civilization—Water Science?* International Association of Hydrological Sciences Publication, **286**, 95–106.

FATELA, F. & TABORDA, R. 2002. Confidence limits of species proportions in microfossils assemblages. *Marine Micropaleontology*, **45**, 169–174.

FERNÁNDEZ-SALAS, L. M., LOBO, F. J., HERNÁNDEZ-MOLINA, F. J., SOMOZA, L., RODERO, J., DÍAZ DEL RÍO, V. & MALDONADO, A. 2003. High-resolution architecture of late Holocene highstand prodeltaic deposits from southern Spain: the imprint of high-frequency climatic and relative sea-level changes. *Continental Shelf Research*, **23**, 1037–1054.

FERRANTI, L., OLDOW, J. S. & SACCHI, M. 1996. Pre-Quaternary orogen-parallel extension in the Southern Apennine belt, Italy. *Tectonophysics*, **260**, 325–347.

FIGLIOLO, B. & MARTURANO, A. 1994. The eruptions of Vesuvius from the 7th to the 12th centuries. *In*: MORELLO, N. (ed.) *Volcanoes and History*. Brigati, Genova, 133–156.

FOLK, R. L. & WARD, W. C. 1957. Brazos river bar: a study in the significance of grain-size parameters. *Journal of Sedimentary Petrology*, **27**, 3–26.

FREY, R. W. & SEILACHER, A. 1980. Uniformity in marine invertebrate ichnology. *Lethaia*, **13**, 183–207.

GILBERT, R. 1975. Sedimentation in Lillooet Lake, British Columbia. *Canandian Journal of Earth Sciences*, **12**, 1697–1711.

GINGRAS, M. K., PEMBERTON, S. G. & SAUNDERS, T. 2001. Bathymetry, sediment texture and substrate cohesiveness; their impact on modern *Glossifungites* trace assemblages at Willapa Bay, Washington. *Palaeogeography, Palaeoclimatology, Palaeoecology*, **169**, 1–21.

GRÉMARE, A., SARDA, R. *ET AL.* 1998. On the dramatic increase of *Ditrupa arietina* O. F. Müller (Annelida: Polychaeta) along both the French and Spanish Catalan coasts. *Estuarine and Coastal Shelf Science*, **47**, 447–457.

HASIOTIS, T., CHARALAMPAKIS, M., STEFATOS, A., PAPATHEODOROU, G. & FERENTINOS, G. 2006. Fan-delta development and processes offshore a seasonal river in a seismically active region, NW Gulf of Corinth. *Geo-Marine Letters*, **26**, 199–211.

HOEFS, J. 1987. *Stable Isotope Geochemistry*. 3rd edn. Springer, Berlin.

HUNT, D. & TUCKER, M. E. 1992. Stranded parasequences and the forced regressive wedge systems tract: deposition during base-level fall. *Sedimentary Geology*, **81**, 1–9.

INSINGA, D. 2003. *Tefrostratigrafia dei depositi tardoquaternari della fascia costiera campana*. PhD thesis, University of Naples Federico II.

INSINGA, D., MOLISSO, F., LUBRITTO, C., SACCHI, M., PASSARIELLO, I. & MORRA, V. 2008. The proximal marine record of Somma–Vesuvius volcanic activity in the Naples and Salerno bays (eastern Tyrrhenian Sea) during the last 3 kyrs. *Journal of Volcanology and Geothermal Research*, **177**, 170–186.

IORIO, M., SAGNOTTI, L. *ET AL.* 2004. High-resolution petrophysical and paleomagnetic study of late-Holocene shelf sediments, Salerno Gulf, Tyrrhenian Sea. *Holocene*, **14**, 433–442.

JORISSEN, F. J. 1987. The distribution of benthic foraminifera in the Adriatic Sea. *Marine Micropalaeontology*, **12**, 21–48.

JORISSEN, F. J. 1988. *Benthic foraminifera from the Adriatic Sea; principles of phenotypic variation*. Utrecht Micropaleontology Bulletin, **37**.

JORISSEN, F. J. & WITTLING, I. 1999. Ecological evidence from live–dead comparison of benthic foraminiferal faunas off Cap Blanc (Northwest Africa). *Palaeogeography, Paleoclimatology, Paleoecology*, **149**, 151–170.

KALLEL, N., PATERNE, M., LABEYRIE, L., DUPLESSY, J. C. & ARNOLD, M. 1997. Temperature and salinity records of the Tyrrhenian Sea during the last 18000 years. *Paleogeography, Paleoclimatology, Palaeoecology*, **135**, 97–108.

LEE, H. J., SYVITSKY, J. P. M., PARKER, G., ORANGE, D., LOCAT, J., HUTTON, J. H. W. & IMRAN, J. 2002. Distinguishing sediment waves from slope failure deposits: field examples, including the 'Humboldt Slide' and modelling results. *Marine Geology*, **192**, 79–104.

LINDSAY, J. F., PRIOR, D. B. & COLEMAN, J. M. 1984. Distributary mouth bar development and role of submarine landslides in delta growth, South Pass, Mississippi Delta. *AAPG Bulletin*, **68**, 1732–1743.

LINKE, P. & LUTZE, G. F. 1993. Microhabitat preferences of benthic foraminifera—a static concept or a dynamic adaptation to optimize food acquisition? *Marine Micropaleontology*, **20**, 215–234.

LIQUETE, C., ARNAU, P., CANALS, M. & COLAS, S. 2005. Mediterranean river systems of Andalusia, southern Spain, and associated deltas: a source to sink approach. *Marine Geology*, **222–223**, 471–495.

LIRER, L., PESCATORE, T. S., BOOTH, B. & WALKER, G. P. L. 1973. Two Plinian pumice-fall deposits from Somma–Vesuvius, Italy. *Geological Society of America Bulletin*, **84**, 759–772.

LIRER, L., VINCI, A., ALBERICO, I., GIFUNI, T., BELLUCCI, F., PETROSINO, P. & TINTERRI, R. 2001. Occurrence of inter-eruption debris-flow and hyperconcentrated flood-flow deposits on Vesuvio volcano, Italy. *Sedimentary Geology*, **139**, 151–167.

LIRER, L., CHIROSCA, M. C., MUNNO, R., PETROSINO, P. & GRIMALDI, M. (eds) 2005. *Il Vesuvio ieri, oggi, domani*. Regione Campania, Naples.

LOBO, F. J., FERNÁNDEZ-SALAS, L. M., MORENO, I., SANZ, J. L. & MALDONADO, A. 2006. The sea-floor morphology of a Mediterranean shelf fed by small rivers, northern Alboran Sea margin. *Continental Shelf Research*, **26**, 2607–2628.

LOEBLICH, A. R. & TAPPAN, H. 1988. *Foraminiferal Genera and their Classification*. Van Nostrand Reinhold, New York.

MACEACHERN, J. A., RAYCHAUDHURI, I. & PEMBERTON, S. G. 1992. Stratigraphic applications of the *Glossifungites* ichnofacies: Delineating discontinuities in the rock record. *In*: PEMBERTON, S. G. (ed.) *Applications of Ichnology to Petroleum Exploration, a Core Workshop*. Society of Economic Paleontologists and Mineralogists, Core Workshops, **17**, 169–198.

MAJOR, J. J., PIERSON, T. C., DIEARTH, R. L. & COSTA, J. E. 2000. Sediment yield following severe volcanic disturbance—A two decade perspective from Mount St. Helens. *Geology*, **28**, 819–822.

MALINVERNO, A. & RYAN, W. B. F. 1986. Extension in the Tyrrhenian Sea and shortening in the Apennines as result of arc migration driven by sinking of the lithosphere. *Tectonics*, **5**, 227–245.

MARIANI, M. & PRATO, R. 1988. I bacini neogenici costieri del margine tirrenico: approccio sismostratigrafico. *Memorie della Società Geologica Italiana*, **41**, 519–531.

MCCONNICO, T. S. & BASSETT, K. N. 2007. Gravelly Gilbert-type fan-delta on the Conway Coast, New Zealand: Foreset depositional processes and clast imbrications. *Sedimentary Geology*, **198**, 147–166.

MILIA, A. & TORRENTE, M. M. 1999. Tectonics and stratigraphic architecture of a peri-Tyrrhenian half-graben (Bay of Naples, Italy). *Tectonophysics*, **315**, 297–314.

MILIA, A., MIRABILE, L., TORRENTE, M. M. & DVORAK, J. J. 1998. Volcanism offshore of Vesuvius volcano in Naples Bay. *Bulletin of Volcanology*, **59**, 404–413.

MILIA, A., MOLISSO, F., RASPINI, A., SACCHI, M. & TORRENTE, M. M. 2008. Syn-eruptive features and sedimentary processes associated with pyroclastic currents entering the sea: the AD 79 eruption of Vesuvius,

Naples Bay, Italy. *Journal of the Geological Society, London*, **165**, 839–848.

MILLER, C. D. 1989. *Potential hazards from future volcanic eruptions in California*. US Geological Survey Bulletin, **1847**.

MILLER, C. D., MULLINEAUX, D. R. & CRANDELL, D. R. 1982. *Potential hazards from future volcanic eruptions in the Long Valley–Mono Lake area, east–central California and southwest Nevada: a preliminary assessment*. US Geological Survey Circular, **877**.

MOSHER, D. C. & SIMPKIN, P. G. 1999. Status and trends of marine high-resolution seismic reflection profiling: data acquisition. *Geoscience Canada*, **26**, 174–187.

MULDER, T. & SYVITSKI, J. P. M. 1995. Turbidity currents generated at river mouths during exceptional discharges to the world oceans. *Journal of Geology*, **103**, 285–299.

MULDER, T., SYVITSKI, J. P. M., MIGEON, S., FAUGÈRES, J.-C. & SAVOYE, B. 2003. Marine hyperpycnal flows: initiation, behavior and related deposits. A review. *Marine and Petroleum Geology*, **20**, 861–882.

MUNNO, R. & PETROSINO, P. 2004. New constraints on the occurrence of Y-3 upper Pleistocene tephra marker layer in the Tyrrhenian Sea. *Quaternario*, **17**, 11–20.

MURRAY, J. W. 1973. *Distribution and Ecology of Living Benthic Foraminiferids*. Cran, Russak, New York.

MURRAY, J. W. 1976. Comparative studies of living and dead benthic foraminiferal distribution. *In*: HEDLEY, R. H. & ADAMS, C. G. (eds) *Foraminifera, 2*. Academic Press, London, 45–109.

MURRAY, J. W. 1991. Ecology and distribution of benthic foraminifera. *In*: LEE, J. J. & ANDERSON, O. R. (eds) *Biology of Foraminifera*. Academic Press, New York, 221–253.

MUTTI, E., TINTERRI, R., BENEVELLI, G., DI BIASE, D. & CAPANNA, G. 2003. Deltaic, mixed and turbidite sedimentation of ancient foreland basins. *Marine and Petroleum Geology*, **20**, 733–755.

NAVA-SANCHEZ, E. H., GORSLINE, D. S., CRUZ-OROZCE, R. & GODINEZ-ORTA, L. 1999. The El Coyote fan-delta: a wave-dominated example from the Gulf of California, Mexico. *Quaternary International*, **56**, 129–140.

NEMEC, W. 1990a. Deltas—remarks on terminology and classification. *In*: COLELLA, A. & PRIOR, D. B. (eds) *Coarse-Grained Deltas*. International Association of Sedimentologists, Special Publications, **10**, 3–12.

NEMEC, W. 1990b. Aspects of sediment movement on steep delta slopes. *In*: COLELLA, A. & PRIOR, D. B. (eds) *Coarse-Grained Deltas*. International Association of Sedimentologists, Special Publications, **10**, 29–73.

NEMEC, W. 1995. The dynamics of deltaic suspension plumes. *In*: OTI, M. N. & POSTMA, G. (eds) *Geology of Deltas*. Balkema, Rotterdam, 31–93.

NEMEC, W. & STEEL, R. J. 1988. What is a fan-delta and how do we recognize it? *In*: NEMEC, W. & STEEL, R. J. (eds) *Fan-Deltas: Sedimentology and Tectonic Settings*. Blackie, Glasgow, 3–13.

OLDOW, J. S., D'ARGENIO, B., FERRANTI, L., PAPPONE, G., MARSELLA, E. & SACCHI, M. 1993. Large-scale longitudinal extension in the southern Apennines contractional belt, Italy. *Geology*, **21**, 1123–1126.

PAPPALARDO, L., CIVETTA, L. *ET AL.* 1999. Chemical and Sr-isotopical evolution of the Phlegrean magmatic system before the Campanian Ignimbrite and the Neapolitan Yellow Tuff eruptions. *Journal of Volcanology and Geothermal Research*, **91**, 141–166.

PARSONS, J. D., BUSH, J. W. M. & SYVITSKI, J. P. M. 2001. Hyperpycnal plume formation from riverine outflows with small sediment concentrations. *Sedimentology*, **48**, 465–478.

PASSARIELLO, I., MARZAIOLI, F. *ET AL.* 2007. Radiocarbon sample preparation at the CIRCE AMS laboratory in Caserta, Italy. *Radiocarbon*, **49**, 225–232.

PATACCA, E. & SCANDONE, P. 2007. Geology of the Southern Apennines. *Bollettino della Società Geologica Italiana, Special Issue*, **7**, 75–119.

PATERNE, M., GUICHARD, F. & LABEYRIE, J. 1988. Explosive activity of the south Italian volcanoes during the past 80 000 years as determined by marine tephrochronology. *Journal of Volcanology and Geothermal Research*, **34**, 153–172.

PEMBERTON, S. G. & FREY, R. W. 1985. The *Glossifungites* ichnofacies: modern examples from the Georgia Coasts, U.S.A. *In*: CURRAN, H. A. (ed.) *Biogenic Structures: their Use in Interpreting Depositional Environments*. Society of Economic Paleontologists and Mineralogists, Special Publications, **35**, 237–259.

PLINK-BJORKLUND, P. & STEEL, R. J. 2004. Initiation of turbidity currents: outcrop evidence for Eocene hyperpycnal-flow turbidites. *Sedimentary Geology*, **165**, 29–52.

PORFIDO, S., ESPOSITO, E., ALAIA, F., MOLISSO, F. & SACCHI, M. 2009. The use of documentary sources for reconstructing flood chronologies on the Amalfi rocky coast (southern Italy). *In*: VIOLANTE, C. (ed.) *Geohazard in Rocky Coastal Areas*. Geological Society, London, Special Publications, **322**, 173–187.

POSAMENTIER, H. W. & ALLEN, G. P. 1993. Variability of the sequence stratigraphic model: effects of local basin factors. *Sedimentary Geology*, **86**, 91–109.

POSTMA, G. 1990. Depositional architecture and facies of river and fan-deltas: a synthesis. *In*: COLELLA, A. & PRIOR, D. B. (eds) *Coarse-Grained Deltas*. International Association of Sedimentologists Special Publications, **10**, 13–27.

POSTMA, G. 1995. Sea-level-related architectural trends in coarse-grained delta complexes. *Sedimentary Geology*, **9**, 3–12.

POSTMA, G., BABIC, L., ZUPANIC, J. & ROE, S. L. 1988. Delta-front failure and associated bottomset deformation in a marine, gravelly Gilbert style fan-Delta. *In*: NEMEC, W. & STEEL, R. J. (eds) *Fan-Deltas—Sedimentology and Tectonic Settings*. Blackie, Glasgow, 91–102.

PRIOR, D. B. & BORNHOLD, B. D. 1990. The underwater development of Holocene fan-deltas. *In*: COLELLA, A. & PRIOR, D. B. (eds) *Coarse-Grained Deltas*. International Association of Sedimentologists, Special Publications, **10**, 75–90.

PRIOR, D. B., BORNHOLD, B. D., WISEMAN, W. J., JR. & LOWE, D. R. 1987. Turbidity current activity in a British Columbia fjord. *Science*, **237**, 1330–1333.

READING, H. G. 1996. *Sedimentary Environments: Processes, Facies and Stratigraphy*. Blackwell Science, Oxford.

REINECK, H. E. & SINGH, I. B. 1975. *Depositional Sedimentary Environments*. Springer, New York.

ROLANDI, G., BARRELLA, A. M. & BORRELLI, A. 1993. The 1631 eruption of Vesuvius. *Journal of Volcanology and Geothermal Research*, **58**, 183–201.

ROLANDI, G., PETROSINO, P. & MCGEEHIN, J. 1998. The inter-Plinian activity at Somma–Vesuvius in the last 3500 years. *Journal of Volcanology and Geothermal Research*, **82**, 19–52.

ROLANDI, G., MUNNO, R. & POSTIGLIONE, I. 2004. The A.D. 472 eruption of the Somma volcano. *Journal of Volcanology and Geothermal Research*, **129**, 291–319.

ROSI, M. & SANTACROCE, R. 1983. The A.D. 472 'Pollena' eruption: volcanological and petrological data for this poorly-known, Plinian-type event at Vesuvius. *Journal of Volcanology and Geothermal Research*, **17**, 249–271.

ROSI, M. & SBRANA, A. (eds) 1987. *Phlegrean Fields*. Quaderni de 'La Ricerca Scientifica', **114**.

ROSI, M., PRINCIPE, C. & VECCI, R. 1993. The 1631 Vesuvius eruption. A reconstruction based on historical and stratigraphic data. *Journal of Volcanology and Geothermal Research*, **58**, 151–182.

SACCHI, M., INFUSO, S. & MARSELLA, E. 1994. Late Pliocene–Early Pleistocene compressional tectonics in offshore Campania (eastern Tyrrhenian Sea). *Bollettino di Geofisica Teorica ed Applicata*, **36**, 141–144.

SACCHI, M., CONFORTI, A., MILIA, A., MOLISSO, F. & VIOLANTE, C. 2004. Il Golfo di Salerno. *In*: ESPOSITO, E., PORFIDO, S. & VIOLANTE, C. (eds) *Il nubifragio dell'Ottobre 1954 a Vietri sul Mare, costa di Amalfi, Salerno. Scenario ed effetti di una piena fluviale catastrofica in un'area di costa rocciosa*. Pubblicazione Gruppo Nazionale per la Difesa dalle Catastrofi Idrogeologiche, **2870**, 45–57.

SACCHI, M., INSINGA, D., MILIA, A., MOLISSO, F., RASPINI, A., TORRENTE, M. M. & CONFORTI, A. 2005. Stratigraphic signature of the Vesuvius 79 AD event off the Sarno prodelta system, Naples Bay. *Marine Geology*, **222–223**, 443–469.

SANTACROCE, R. (ed.) 1987. *Somma–Vesuvius. Quaderni de 'La Ricerca Scientifica'*.

SANTACROCE, R. & SBRANA, A. 2003. *Carta Geologica del Vesuvio*. Progetto CARG-Carta Geologica d'Italia, Servizio Geologico d'Italia. SELCA, Firenze.

SANTACROCE, R., SULPIZIO, R. *ET AL.* 2008. Age and whole rocks–glass composition of proximal pyroclastics from the major explosive eruptions of Vesuvius: a review as a tool for distal tephrostratigraphy. *Journal of Volcanology and Geothermal Research*, **177**, 1–18.

SCHMIEDL, G., DE BOVÉE, F., BUSCAIL, R., CHARRIÈRE, B., HEMLEBEN, C., MEDERNACH, L. & PICON, P. 2000. Trophic control of benthic foraminiferal abundance and microhabitat in the bathyal Gulf of Lions, western Mediterranean *Sea. Marine Micropaleontology*, **40**, 167–188.

SGARRELLA, F. & BARRA, D. 1984. Distribuzione dei foraminiferi bentonici nel Golfo di Salerno (Basso Tirreno, Italia). *Bollettino della Società dei Naturalisti Napoli*, **93**, 1–58.

SGARRELLA, F. & MONTCHARMONT-ZEI, M. 1993. Benthic foraminifers of the Gulf of Naples (Italy): systematics and autoecology. *Bollettino della Società Paleontologica Italiana*, **32**, 145–264.

SIANI, G., SULPIZIO, R., PATERNE, M. & SBRANA, A. 2004. Tephrostratigraphy study for the last 18,000 ^{14}C years in a deep-sea sediment sequence for the South *Adriatic. Quaternary Science Review*, **23**, 2485–2500.

SIGURDSSON, H., CAREY, S., CORNELL, W. & PESCATORE, T. 1985. The eruption of Vesuvius in AD 79. *National Geographic Research*, **1**, 332–387.

SIMPKIN, P. G. & DAVIS, A. 1993. For seismic profiling in very shallow water, a novel receiver. *Sea Technology*, **34**, 21–28.

SULPIZIO, R., MELE, D., DELLINO, P. & LA VOLPE, L. 2005. A complex sub-Plinian-type eruption from low-viscosity, phonolitic to tephri-phonolitic magma: the AD 472 (Pollena) eruption of Somma–Vesuvius, Italy. *Bulletin of Volcanology*, **67**, 743–767.

SULPIZIO, R., ZANCHETTA, G., DEMI, F., DI VITO, M., PARESCHI, M. T. & SANTACROCE, R. 2006. The Holocene syneruptive volcaniclastic debris flow in the Vesuvian area: geological data as a guide for hazard assessment. *In*: SIEBE, C., MACIAS, J. L. & AGUIRRE-DIAZ, G. J. (eds) *Neogene–Quaternary Continental Margin Volcanism: a Perspective from Mexico*. Geological Society of America, Special Papers, **402**, 203–221.

SULTAN, N., COCHONAT, P. *ET AL.* 2004. Triggering mechanisms of slope instability processes and sediment failures on continental margins: a geotechnical approach. *Marine Geology*, **213**, 291–321.

TRINCARDI, F. & SYVITSKI, J. P. M. 2005. Advances on our understanding of delta/prodelta environments: A focus on southern European margins. *Marine Geology*, **222–223**, 1–5.

TRINCARDI, F., CATTANEO, A., CORREGGIARI, A. & RIDENTE, D. 2004. Evidence of soft sediment deformation, fluid escape, sediment failure and regional weak layers within the late Quaternary mud deposits of the Adriatic Sea. *Marine Geology*, **213**, 91–119.

VEZZOLI, L. (ed.) 1988. *Island of Ischia*. Quaderni de 'La Ricerca Scientifica', **114**.

VIOLANTE, C. 2009. Rocky coast: geological constraints for hazard assessment. *In*: VIOLANTE, C. (ed.) *Geohazard in Rocky Coastal Areas*. Geological Society, London, Special Publications, **322**, 1–31.

VIOLANTE, C., BISCARINI, C., ESPOSITO, E., MOLISSO, F., PORFIDO, S. & SACCHI, M. 2009. The consequences of hydrologic events on steep coastal watersheds: the Costa d'Amalfi, eastern Tyrrhenian sea. *In*: LIEBSHER, H. J. *ET AL.* (eds) *The Role of Hydrology in Water Resource Management. Capri Italy, 2008*. IAHS Publication, **327**, 102–113.

VOGEL, J. S., SOUTHON, J. R., NELSON, D. E. & BROWN, T. A. 1984. Performance of catalytically condensed carbon for use in accelerator mass spectrometry. *Nuclear Instruments and Methods*, **B5**, 289–293.

WENINGER, B. & JÖRIS, O. 2007. A ^{14}C age calibration curve for the last 60 ka: the Greenland-Hulu U/Th

timescale and its impact on understanding the Middle to Upper Paleolithic transition in Western Eurasia. *Journal of Human Evolution*, **55**, 772–781.

WENINGER, B., JÖRIS, O. & DANZEGLOCKE, U. 2008. CalPal-2007. Cologne Radiocarbon Calibration & Palaeoclimate Research Package. World Wide Web Address: http://www.calpal.de/

WESCOTT, W. A. & ETHRIDGE, F. G. 1990. Fan-deltas—Alluvial fans in coastal settings. *In*: RACHOCKI, A. H. & CHURCH, M. (eds) *Alluvial Fans: a Field Approach.* Wiley, New York, 195–211.

WULF, S., KRAML, M., BRAUER, A., KELLER, J. & NEGENDANK, J. F. W. 2008. Tephrochronology of the 100 ka lacustrine sediment record of Lago Grande di Monticchio (southern Italy). *Journal of Volcanology and Geothermal Research*, **177**, 118–132.

WULF, S., KRAML, M., BRAUER, A., KELLER, J. & NEGENDANK, J. F. W. 2004. Tephrochronology of the 100 ka lacustrine sediment record of Lago Grande di Monticchio (southern Italy). *Quaternary International*, **122**, 7–30.